12-2013

Environmental constraints on cyanomyophage abundance in the subtropical Pacific Ocean

Tiana Maria Pimentel
University of Tennessee - Knoxville, tpimente@utk.edu

To the Graduate Council:

I am submitting herewith a thesis written by Tiana Maria Pimentel entitled "Environmental constraints on cyanomyophage abundance in the subtropical Pacific Ocean." I have examined the final electronic copy of this thesis for form and content and recommend that it be accepted in partial fulfillment of the requirements for the degree of Master of Science, with a major in Microbiology.

Steven W. Wilhelm, Major Professor

We have read this thesis and recommend its acceptance:

Erik R. Zinser, Alison Buchan

Accepted for the Council:
Carolyn R. Hodges

Vice Provost and Dean of the Graduate School

(Original signatures are on file with official student records.)

Environmental constraints on cyanomyophage abundance in the subtropical Pacific Ocean

A Thesis Presented for the

Master of Science

Degree

The University of Tennessee, Knoxville

Tiana Maria Pimentel

December 2013

ACKNOWLEDGEMENTS

None of this would have been possible without the help of so many. First of all, I would like to thank my advisor Dr. Steven Wilhelm for his support and mentorship throughout this project. His wisdom and patience are unmatched, and no one is better at calming down graduate students who are in mid-crisis. Also, he has excellent taste in British television, and I couldn't have done any of this without him (or The Doctor). I must extend my deepest gratitude to our collaborators in Dr. Zackary Johnson's lab at Duke University as well for collecting a great portion of the data I used in my thesis research, and to my committee members Dr. Erik Zinser and Dr. Alison Buchan for their input in the shaping of this project. Their expertise was invaluable to me throughout my time here at the University of Tennessee.

Thanks are due to all of the members of the 6th floor of SERF, but especially to Alise Ponsero, Jackson Gainer, and Jeremy Chandler. I will always be grateful to them for their friendship and for their sense of humor in the face of crippling boredom aboard the POWOW1 cruise. Also, I owe a great deal to Dr. Gary LeCleir for his advice and assistance, as well as to Dr. Drew Steen for helping me to understand the joys of R programming.

Finally, thank you to all my family and non-science friends for their support, but especially to my Mom and my grandparents. Their love and patience helped me keep going when all I wanted to do was quit, and for that I am extremely grateful. Last, but certainly not least, I would like to thank my best friend and cheerleader, Nick, for making me laugh even when I was miserable and for helping me to see that I had it in me all along. I would not be the same person I am today without you.

ABSTRACT

Viruses are abundant in the world's oceans and are thought to be important participants in marine biogeochemical cycling. Of these viruses, cyanophages are considered especially important because they infect and lyse cyanobacteria, which are some of the main primary producers in marine environments. Cyanophages are thought to influence the abundance and diversity of cyanobacterial populations and impart significant mortality, thereby affecting primary productivity and microbial community structure. Despite their ecological relevance, little is known about how environmental factors shape cyanophage abundance and diversity over large temporal and spatial scales. To address this gap in knowledge, seawater samples were collected during a research cruise transect from Honolulu, HI to San Diego, CA. The *Myoviridae* family of cyanophage was targeted for this study because of its perceived ecological dominance and the availability of molecular probes which can be used to measure their diversity and quantify abundance. The *g20* gene (which codes for portal vertex protein in myoviruses) was targeted by an established primer set and used as a proxy for cyanomyophage abundance in qPCR assays. Initial analysis of quantification data has revealed significant correlations between cyanomyophage abundance and depth, dissolved inorganic carbon concentration, and total viral abundance. Total viral abundance was also significantly correlated with depth. The lack of trends between viral abundance and other environmental variables may have been due to the temporal offset in the phage-host relationship, which needs to be taken into consideration in future studies.

TABLE OF CONTENTS

LIST OF TABLES

LIST OF FIGURES

LIST OF ABBREVIATIONS

- ALOHA, A Long-term Oligotrophic Habitat Assessment
- AU, arbitrary unit
- BDL, below detection limits
- bp, base pair
- CTD, conductivity, temperature, depth
- DIC, dissolved inorganic carbon
- dNTP, deoxyribonucleotide triphosphates
- DOM, dissolved organic matter
- dsDNA, double-stranded DNA
- FCM, flow cytometry
- FU, fluorescence units
- LMP, low melting point
- Mbp, megabase pairs
- MPN, most probable number
- PA, plaque assay
- PAR, photosynthetically active radiation
- PBS, phosphate buffered saline
- PCR, polymerase chain reaction
- POWOW1, Phytoplankton of Warming Ocean Waters, cruise 1
- PSII, photosystem II
- qPCR, quantitative polymerase chain reaction
- SD, standard deviation
- TE, tris-ethylenediaminetetraacetic acid
- TFF, tangential flow filtration
- UV, ultraviolet
- UW, underway
- VLP, virus-like particles

I. INTRODUCTION

Importance of marine viruses

Viruses are the most abundant biological entities in aquatic systems and have been documented at densities up to 10^8 virus-like particles (VLP) mL^{-1} (Bergh et al. 1989, Bratbak et al. 1990, Proctor & Fuhrman 1990, Wilhelm & Suttle 1999). Typically, marine viral abundances are lower than those reported for freshwater systems (Suttle 2005, Wilhelm & Matteson 2008). Even so, estimates suggest that there are ~10^{30} total VLP in the world's oceans (Suttle 2005). To put this astronomically high number into perspective, Suttle (2005) calculated that if all the marine viruses were lined up end to end, the chain would span ~100 million light years (assuming an average viral length of 100 nm). It has been widely theorized that a majority of marine virioplankton are bacteriophages due to the correlation between bacterial and viral abundances across studies and the fact that viruses outnumber bacteria by at least by an order of magnitude or more in most aquatic environments (Borsheim 1993, Wilhelm & Matteson 2008)..

Participation in biogeochemical cycling and shaping of host communities

Recently, there has been increased interest in determining the role of bacteriophage in ecosystem functioning. Phage are thought to contribute to marine biogeochemical cycles by releasing bioavailable carbon and nutrients as dissolved organic matter (DOM) through the infection and lysis of their hosts (Wilhelm & Suttle 1999, Brussaard et al. 2008). This lytic activity results in a shuttling of carbon from "higher" trophic levels to the dissolved pool; a process referred to as the "viral shunt" (Wilhelm & Suttle 1999). The percentage of bacterial carbon which is released *via* the viral shunt has been estimated to be between 8-42% in offshore and 6.8-25% in near-shore marine environments – on par with the effects of grazing (Wilhelm &

Suttle 1999). Viruses are also implicated in the termination of algal blooms (Bratbak et al. 1990), demonstrating their potential to control host populations on a massive scale. Thus, viral infection is theorized to be an important cause of prokaryotic mortality in marine environments.

Bacteriophage are assumed to "select" their hosts through a "kill the winner" mechanism, in which the most dominant microbes are more likely to succumb to viral infection due to increased contact rates, enabling less dominant members of the community to flourish (Thingstad et al. 1993, Thingstad & Lignell 1997). Through this process, phage influence microbial community structure (Muhling et al. 2005, Rodriguez-Brito et al. 2010) and genetic diversity within potential host populations (Weinbauer & Rassoulzadegan 2004, Sandaa et al. 2009). Evidence suggests that this selection process is the product of a constant evolutionary arms race between phages and their hosts – hosts evolving to become resistant while new viruses evolve to infect those host – a microbial manifestation of Red Queen Theory (Valen 1973, Wilhelm and Matteson 2008) This continual evolution of the community results in the generation of many phage-resistant bacteria (Waterbury & Valois 1993, Stoddard et al. 2007). However, the generation of resistance is thought to be associated with a decrease in fitness, which may promote reversions back to susceptible states in aquatic environments (Lennon et al. 2007, Marston et al. 2012).

Cyanophage

Cyanophage (*i.e.*, viruses that infect cyanobacteria) were first isolated from fresh waters in the 1960's (Safferman & Morris 1963) and have since been found in nearly every aquatic system studied to date (Moisa et al. 1981, Suttle & Chan 1993, Waterbury & Valois 1993, Suttle & Chan 1994). The picocyanobacteria *Synechococcus* and *Prochlorococcus* are the dominant

primary producers in the ocean, together providing around 25% of global photosynthesis (Partensky et al. 1999), and thus the cyanophage which infect them are historically the most widely studied of the marine viruses. Cyanophage reduce primary productivity by inducing lysis of their cyanobacterial hosts (Proctor & Fuhrman 1990, Suttle et al. 1990). This influence of cyanophage infection on primary production has been termed "side-in" control (Bratbak et al. 1993b), though recently the term "top-down" control has become more widely used (Weinbauer & Hofle 1998, Zhao et al. 2013). The percentage of *Synechococcus* infected on a daily basis has been estimated to be in the range of around 2% - 10% in certain marine environments (Suttle & Chan 1994, Wang et al. 2011), while others have come up with percentages as high as 46% (Matteson et al. 2013).

In many cases, cyanophage have been known to have genes within their genomes that appear to be of host origin (Mann 2003, Lindell et al. 2004, Millard et al. 2004, Sharon et al. 2009). Not only do these genes have the potential to participate in horizontal gene transfer, thus contributing to host diversity, but evidence also shows that some of these genes are active during infection and may give phage an adaptive advantage (Lindell et al. 2005, Clokie et al. 2006, Sharon et al. 2009, Thompson et al. 2011). During infection, the cyanobacterial host blocks the transcription and translation of host genes as a defense mechanism against phage proliferation (Sherman & Pauw 1976, Schneider & Shenk 1987, Rohwer & Thurber 2009). It has also been demonstrated that the *Synechococcus* phage AS-1 can degrade the host genome within an hour after a successful infection (Sherman & Pauw 1976). Without intervention, photosynthesis is gradually shut down under infection conditions because rapid-cycling photosynthesis proteins, such as the photosystem II (PSII) D1 protein, are steadily depleted (Lindell et al. 2005).

However, cyanophage encode and produce proteins from their own hijacked versions of these genes, called "host auxiliary genes," perhaps allowing photosynthesis to continue unhindered during infection (Lindell et al. 2005, Clokie et al. 2006). Also, it has been demonstrated that cyanophages can use host auxiliary gene products to redirect host metabolism towards pathways which are more favorable to phage proliferation, such as from carbon fixation towards dNTP synthesis (Thompson et al. 2011). Thus, cyanophage alter their host's contribution to biogeochemical cycling in life as well as through cell lysis.

Dominance of cyanomyoviruses in aquatic systems

To date, most marine phage isolates and all cyanophage isolates belong to the order *Caudovirales*, or "tailed viruses" (Borsheim 1993). The tailed viruses are divided into three families, *Siphoviridae*, *Podoviridae*, and *Myoviridae*, which are differentiated based on morphology (Maniloff & Ackermann 1998). Though representatives from all three families have been demonstrated to infect cyanobacteria, the most frequently isolated cyanophage are members of the family *Myoviridae* (Suttle & Chan 1993, Waterbury & Valois 1993). Myoviruses are distinguished by their icosahedral capsids and contractile tails (Maniloff & Ackermann 1998). The family *Myoviridae* is subdivided into six genera, but most isolated cyanophage fall into the "T4-like" phages (Sullivan et al. 2010), which are known to be primarily lytic (Maniloff & Ackermann 1998). All T4-like myoviruses have a core genome consisting of 38 genes, but cyanophages in this genera have a unique set of 25 core genes which distinguish them from myoviruses that infect other hosts (Sullivan et al. 2010). Unfortunately, the other two cyanophage families do not share any core genes with the cyanomyoviruses, so they must be studied separately when molecular methods are to be used (Paul et al. 2002). The

cyanopodoviruses have some core genes (Sullivan et al. 2005), and primers have been developed which target their DNA polymerase gene for use in phylogenetic studies (Labonte et al. 2009). However, no primers have been developed for quantitative assays of cyanopodoviral abundance. The *Siphoviridae* possess no core genes to target for molecular studies (Sullivan et al. 2009, Huang et al. 2012).

Myoviruses are popularly considered the most dominant family of cyanophage because they have a broad host range (Suttle & Chan 1993, Waterbury & Valois 1993), and are the most commonly isolated in the laboratory (Mann 2003, Weinbauer 2004), which may be a product of their broad host range rather than their prevalence in the environment. However, it was also found that a cyanomyoviral marker gene was highly prevalent in both the Sargasso Sea and the South Pacific Ocean (Matteson et al. 2013). Moreover, T4-like myoviral genes are frequently identified in oceanic metagenomic surveys (Rusch et al. 2007, Yooseph et al. 2007). Since myoviral molecular markers appeared in the microbial fractions in these studies (which should have excluded any free floating viral particles and only included ones inside or intimately associated with host bacteria), this suggests that not only are myoviruses extremely common, but they are actively infectious.

Historically, the abundance of cyanophage has been determined using most probable number assays (MPN) and plaque assays (PA); both of which require the propagation of natural viral samples on certain hosts (Waterbury & Valois 1993, Suttle & Chan 1994, Garza & Suttle 1998, Sullivan et al. 2003, Millard & Mann 2006, Wang et al. 2011). Marine cyanophage abundances determined through these techniques range from undetectable to ~10^5 cyanophage mL^{-1} (Table 1). However, since no universally permissive host has been identified, these assays

likely underestimate the abundance of infectious cyanophage in aquatic environments (Waterbury & Valois 1993). Recently, a qPCR protocol has been optimized which enables the quantification of the *g20* gene as a proxy for cyanomyoviral abundance (Matteson et al. 2011). This method has been used previously to demonstrate the high abundance of cyanomyophage in both freshwater and marine systems (Sandaa & Larsen 2006, Matteson et al. 2011, Matteson et al. 2013), and though it only targets one cyanophage family, it avoids the problem of identifying a universally permissive host, which most likely does not exist. A comparison of the cyanophage abundances obtained from culture-based and molecular methods are shown in Table 1. Though some abundances obtained from MPN assays are close to those found using the molecular method (in the realm of 10^5 cyanophages mL^1), it must be noted that the two methods have not yet been used in tandem on the same samples, so it is not possible to draw conclusions about how they compare except on a theoretical standpoint.

The current qPCR protocol to examine cyanomyoviruses employs the same forward primer employed in numerous studies of cyanomyophage genetic richness (Fuller et al. 1998, Zhong et al. 2002, Muhling et al. 2005, Wilhelm et al. 2006, Sullivan et al. 2008, Wang et al. 2010), providing an overlap with known phylogenies. This protocol enables the amplification of around 80% of the *g20* genes found in known cyanomyoviral isolates (Zhong et al. 2002). One caveat is that the primers used in these studies are under scrutiny because phylogenetic trees assembled from environmental *g20* gene amplicons produce some clades with no isolated cyanomyoviral representatives, suggesting that they may also amplify T4-like myoviruses infecting non-cyanobacterial hosts (Sullivan et al. 2003, Short & Suttle 2005, Wilhelm et al. 2006). On the other hand, no isolated T4-like myoviruses infecting other hosts have produced

g20 amplicons through the use of this assay (Zhong et al. 2002) and so far, no alternative source for this genetic material has been positively identified, suggesting that these primers likely target only cyanomyoviruses (Matteson et al. 2011). Furthermore, molecular methods producing amplicons in clades without cultured representatives are used frequently, and it is not uncommon for representatives from these clades to be identified and cultured later on (Stingl et al. 2007). Though these cyanomyophages are widely studied in terms of phylogenetic diversity, only a few studies have investigated how ecological factors affect their abundance over large geographical areas.

Table 1. Comparison of cyanophage abundance estimates across studies using differential quantitative methods. Only the highest recorded abundance for each study is reported. In the method column, PA = plaque assay, MPN = most probable number assay, *g20* = qPCR targeting cyanomyoviral *g20* gene. Culture-based assays (MPN and PA) propagated phage on several strains of cyanobacteria in the genus indicated (*Syn.* = *Synechococcus*, *Pro.* = *Prochlorococcus*). It should be noted that the qPCR method calculates the total cyanomyoviral abundance (infectious and inactivated), while the other methods determine the abundance of cyanophage that infect the chosen host(s) (of all cyanophage families).

Max. Abundance	Method	Hosts	Environment	Source
$>10^3$ VLPs mL^{-1}	PA	*Syn.*	Gulf of Mexico and Arkansas Pass	Suttle & Chan, 1994
$>10^4$ VLPs mL^{-1}	MPN	*Syn.*	Coastal and Oligotrophic marine	Waterbury & Valois, 1993
$>10^5$ VLPs mL^{-1}	MPN	*Syn.*	Gulf of Mexico	Garza & Suttle, 1998
$>10^5$ VLPs mL^{-1}	MPN	*Syn.*	Chesapeake Bay	Wang et al., 2011
$>10^3$ VLPs mL^{-1}	MPN	*Syn.* & *Pro.*	Coastal and Oligotrophic Atlantic	Sullivan et al., 2003
$>10^6$ copies mL^{-1}	*g20*	-	Lake Erie	Matteson et al., 2011
$>10^5$ copies mL^{-1}	*g20*	-	South Pacific	Matteson et al., 2013
$>10^3$ copies mL^{-1}	*g20*	-	Norwegian Coast	Sandaa & Larsen, 2006

Ecological conditions affecting viral abundance and activity

The *in situ* viral abundance in the ocean is the result of the production and degradation/inactivation of viral particles (Weinbauer et al. 1999, Wilhelm & Suttle 1999). Since viral abundance remains relatively constant over long periods of time, logically, the rate of viral production must be in balance with the rate of removal to maintain the steadily high abundances observed in aquatic environments (Wilhelm et al. 1998). Evidence suggests that environmental factors may also play a role in both destructive and productive viral processes (Suttle & Feng 1992, Noble & Fuhrman 1997, Bongiorni et al. 2005, Danovaro et al. 2011), thus possibly influencing the total abundance of viruses in aquatic environments. Evidence also suggests that the constraints on viral abundance differ between disparate environments (Danovaro et al. 2011, Rowe et al. 2012). However, research on how environmental parameters affect the abundance of individual phage families in aquatic environments is largely lacking, as most existing data focus on total viral abundance (Matteson et al. 2013). Considering the monumental diversity housed within marine phages (Suttle 2005), there could be any number of variables acting on each specific group, thus obscuring the interactions taking place when observed from a total population standpoint. Therefore, determining the abundance and activities of distinct phage families in different ecological conditions may be crucial to understanding phage ecology.

Since cyanophages are obligate parasites, it makes sense that cyanophage abundances should correlate with cyanobacterial production and abundance more readily than other environmental variables (Suttle 2000). In fact, some studies have found correlations between total viral abundance and cyanobacterial abundances over long time spans in marine environments (Yang et al. 2010, Parsons et al. 2012). Some environmental studies have shown

similar relationships between cyanophage and their hosts, uncovering positive correlations between host abundance and productivity with total cyanophage and cyanomyoviral abundance (Suttle & Chan 1994, Matteson et al. 2013). However, this relationship is complicated by the temporal nature of the host-phage dynamic. In the model proposed by Wommack and Colwell (2000), epidemic phage infection happens shortly after host abundance has reached its peak, causing a lag period, subsequent drop-off in host abundance, and increase in phage abundance. Matteson et al. (2012) observed this offset during a phytoplankton bloom in the South Pacific Ocean, where the activity of the total viral community lagged 24 hours behind that of the bacterial community. Since the phage-host relationship is out of sync temporally, environmental parameters may prove to be better predictors of phage abundance in the environment if they do indeed influence viral dynamics.

Evidence of environmental control on cyanophage abundance

Studies have shown that total viral abundance is low both in oligotrophic waters farther from shore and deeper in the water column (Weinbauer 2004, Suttle 2005). Cyanophage abundances seem to vary in a similar manner. For example, in an MPN-based study in the Gulf of Mexico, cyanophage abundance decreased with increasing distance from shore and depth (Suttle & Chan 1994). Interestingly, in this same study it was shown that *Synechococcus* cells from offshore stations were more susceptible to cyanophage infection. The lower abundances of cyanophage probably resulted in decreased contact rates between host and phage, thus the selective pressure for resistance was much less pronounced farther from shore (Suttle & Chan 1994). This may be one reason cyanophage can persist in oligotrophic waters despite lower host abundances (Suttle & Chan 1994). The effect of depth on cyanophage abundance is likely a

function of the availability of photosynthetically active radiation (PAR) for photosynthesis. However, cyanophage proliferating at depths with high PAR availability are subject to higher doses of UV radiation (Llabres et al. 2010), which causes phage inactivation (Weinbauer et al. 1999). It has been found that UV-related phage decay rates are high at the surface and decrease with increasing depth (Garza & Suttle 1998, Weinbauer et al. 1999), perhaps allowing phage to persist at deeper depths for longer periods of time. This also necessitates that cyanophage in surface waters must be rapidly replaced to balance out UV-related decay rates and sustain the high abundances observed there. Though cyanophage abundance has been found to have an inverse relationship with depth, few studies have collected cyanophage abundances below the first 25 m of the water column.

Some evidence exists to support the idea that phosphate is a limiting factor to cyanophage growth; for example, it was demonstrated previously that phosphate limitation caused decreased burst sizes and increased latency periods in three specific cyanomyophages (S-PM2, S-WHM1, and S-BM1) infecting *Synechococcus* WH7803 (Wilson et al. 1996). Similarly, it was shown that phosphate limitation dramatically inhibited the production of viruses infecting *Emiliania huxleyi*, a marine coccolithophorid (Bratbak et al. 1993a). However, nitrate limitation had virtually no effect on viral production in the same study, which is interesting, considering nitrogen is one of the most common limiting nutrients in marine environments (Eppley et al. 1973). Cyanophages have also been known to encode genes involved in phosphate acquisition, some of which are more active during infection in phosphate limited environments (Zeng & Chisholm 2012). It is theorized that phosphate may be influential in viral proliferation because there would be a high demand for the molecule during the manufacture of nucleic acids (Wilson et al. 1996).

Higher temperature waters have been associated with higher viral decay rates (Garza & Suttle 1998). However, it was demonstrated that cyanophage concentration was greatest in higher temperature waters in the Gulf of Mexico (Suttle & Chan 1994). Viral abundance seems to vary predictably with the seasons, with higher numbers during the summer and spring and declining numbers in the fall and winter (Waterbury & Valois 1993, Suttle & Chan 1994, McDaniel et al. 2002, Wang & Chen 2004). This correlates well with temperature changes, but also with other parameters that vary seasonally, such as host abundance and productivity. However, temperature seems to have differing effects on viral abundance depending on the geographical region being studied (Danovaro et al. 2011), and some areas reveal no obvious relationship between temperature and cyanophage abundance (Matteson et al. 2013), suggesting complex relationships exist between cyanophage and the environment.

II. RESEARCH OBJECTIVES

To date, most studies of virus abundance and distribution have focused on the total viral community (i.e., virus particles determined *via* direct counts) rather than on individual populations. Though it is useful to monitor community behavior, this approach overlooks the contributions of individual virus genotypes or groups, which may react uniquely to environmental changes, resulting in an incomplete understanding of viral ecological functions. Considering the perceived vast diversity of marine viruses, it is both an important and daunting task to assess the distribution of specific viral families in various environmental conditions. There is also a dearth of information on viral dispersal over large geographical and temporal scales. To this end, we investigated the abundance of cyanomyoviruses over a transect in the Pacific Ocean spanning the region from Hawaii to the California coast. This transect traversed a temperature gradient, allowing samples to be collected over a wide range of temperatures in both coastal and oligotrophic ocean waters. As previous research indicated that environmental factors have differential effects on total phage abundance, we proposed the following main hypothesis and sub-hypotheses:

Hypothesis: Environmental factors affect cyanophage abundance in the Pacific Ocean -

1. **Cyanophage abundance increases with water temperature**
2. **Cyanophage abundance is highest at the surface and decreases with depth.**
3. **Waters with higher phosphate concentrations have higher cyanophage abundance.**

To investigate these hypotheses, we completed the following research objectives:

- Water samples were collected on a transect from Hawaii to San Diego (CA) to sample across a series of temperature and geochemical regimes.
- Flow cytometry, epifluorescence microscopy, and qPCR were performed to obtain host, total viral, and cyanomyophage abundances (respectively).
- Marine physiochemical measurements were recorded along the transect (temperature, salinity, pH, nutrient concentrations).
- Statistical analyses were applied to assess relationships between biological and chemical parameters.

All bacterial and cyanobacterial abundances, nutrient concentrations, and pH measurements were collected by members of Dr. Zackary Johnson's lab (Duke University, Durham, NC). Epifluorescence microscopy and qPCR counts were conducted by me with some assistance from Alise Ponsero (CEA Saclay, France). The R scripts for processing data, exploring environmental relationships, and generating figures were written by me with a lot of help from Dr. Drew Steen (University of Tennessee – Knoxville, Knoxville, TN).

III. METHODS

Collection of field samples

The POWOW1 (Phytoplankton of Warming Ocean Waters) cruise was conducted between March 1 (Julian day 61) and March 11 (Julian day 70), 2012] aboard the R/V *Thomas G. Thompson* (cruise track shown in Fig. 1). Depth profile samples for viral counts and qPCR analysis were collected at the surface (*c.* 3-4 m), 25 m, 100 m, 300 m, and the deep chlorophyll maximum (DCM) (*c*. 5:30 am, local time) from the rosette sampler using Niskin bottles. Samples for nutrient concentrations, flow cytometry counts, chlorophyll α concentrations, and measures of acidity were collected at 0 m, 15 m, 25 m, 50 m, 75 m, 100 m, 125 m, 150 m, 175 m, 200 m, and the DCM in the same manner. Depth, temperature, salinity, and *in situ* fluorescence were recorded by the ship's CTD (conductivity, temperature, depth) package attached to the rosette sampler. The DCM was determined daily as the depth with maximum *in situ* fluorescence. Bottles for sample collection were rinsed vigorously three times with MilliQ water, dried overnight, and then rinsed three times with seawater from the appropriate depth immediately prior to sample collection. Underway samples were collected daily in sterile polycarbonate bottles (*c.* 1:00 pm, local time) from the ship's clean surface pump (*c.* 5 m) starting after station 4. Temperature, salinity, and coordinates for underway samples were recorded from ship-board sensors.

Nutrient concentrations

All nutrient concentrations were measured by Dr. Zackary Johnson's group (Duke University, Durham, NC). Ammonium (NH_4) was measured in unfiltered samples on-board the *Thompson* following Holmes et al. (1999). Samples for DIC concentration determination were

collected following procedures detailed in Dickson et al. (2007). The DIC concentration was measured in mercuric chloride poisoned samples which were subjected to acidification. The subsequent release of CO_2 was measured with a CO_2 detector (Li-Cor 7000) and measurements were calibrated against Certified Reference Materials (provided by Dr. A.G. Dickson at Scripps Institution of Oceanography, University of California San Diego).

Water samples for all other nutrient analyses (NO_2, NO_3, PO_4, $SiOH_4$) were collected in HCl-cleaned HDPE bottles (VWR#414004-110) and stored at -80°C before processing. Nutrient concentrations were determined from duplicate samples run on an Astoria-Pacific A2 autoanalyzer following the manufacturer's recommended protocols. Certified reference materials were used to verify protocols (Inorganic Ventures: QCP-NT, QCP-NUT-1, CGSI1-1). The detection limits for each nutrient were 0.05 μM (PO_4 and NO_2), 0.2 μM ($SiOH_4$), 9.0 nM (NH_4), and 0.1 μM (NO_3). Sample concentrations were reported as BDL (below detection limits) if the mean fell below quantifiable limits.

qPCR *g20* quantification

Plasmid standards for qPCR were made from PCR-amplified *g20* from *Synechococcus* S-PWM1 phage with CPS1 and CPS8 primers as previously reported (Zhong et al. 2002, Matteson et al. 2013). Amplicons were cloned into a TOPO-TA pCR 2.1-TOPO cloning vector according to the product manual (Invitrogen, Carlsbad, CA). Plasmids were purified using the Qiaprep Spin Miniprep kit (Qiagen, Valencia, CA). Clones were verified *via EcoRI* digestion, gel electrophoresis, and sequencing by the University of Tennessee Molecular Biology Resource Facility. The plasmid DNA concentration and quality ($A_{260/280}$) were measured with a NanoDrop® ND-1000 Spectrophotometer (Thermo Scientific, Waltham, MA). The molecular

weight of each plasmid and insert was determined using OligoCalc (ver. 3.26) (Kibbe 2007). Avogadro's number was used to determine standard plasmid copies per μL (6.022×10^{23} plasmid copies mol^{-1}). Standards were freshly diluted from a plasmid stock stored at -80° C in TE buffer. Each standard qPCR reaction contained between 10^2 and 10^5 copies per reaction. Reactions were run in low-profile 96-well plates (Bio-Rad, Hercules CA) and sealed with optically clear flat 8-cap strips (Thermo Scientific). Standards were run in duplicate or triplicate and assayed with at least five different dilutions to generate a linear standard curve.

Samples for qPCR analysis were flash frozen in liquid nitrogen. Once transported back to the lab, the samples were transferred to a freezer and stored at -80° C until processed. The qPCR protocol followed details in Matteson et al. (2011). Prior to qPCR quantification, samples were subjected to ultracentrifugation at 90,000-100,000 x **g** for 3 hours at 4° C (Sorvall WX Ultra 80, Thermo Scientific). Pelleted samples were resuspended in 25 μL sterile water and stored at -20° C until use. Since pelleted samples always contained a small amount of additional seawater, the actual resuspended volume was determined through pipetting. Each plate was run on an Opticon 2 Real-Time PCR Detector (BIO-RAD) with triplicate wells containing a known number of intact S-PWM1 phage particles (quantified via epifluorescence microscopy as described later in the methods) for on-going standard verification. All plates yielded acceptable estimates of S-PWM1 abundance. Environmental samples were quantified in triplicate across three ten-fold dilutions. PCR inhibition and recovery for this assay was assessed previously (Matteson et al. 2013). Each 25 μL reaction contained 5 μL sample or standard, 12.5 μL Thermo Scientific Absolute SYBR Green QPCR mix (Thermo Scientific, Waltham, MA), 280 ng μL^{-1} bovine serum albumin (BSA) (Fisher Scientific), 0.30 μM CPS1 forward and 0.60 μM CPS2 reverse

primers (both HPLC purified by Eurofins MWG Operon, Huntsville, AL). Plates loaded with template and master mix were centrifuged at 1700 x **g** at room temperature for 2 min prior to each qPCR reaction in a benchtop centrifuge (Sorvall Legend RT, Thermo Scientific).

PCR conditions consisted of an initial denaturation step at 95° C for 15 min followed by 35 cycles of 95° C for 10 s, 53° C for 30 s, and 72° C for 30 s, with fluorescence quantified at the end of each cycle. A second plate read at 77° C was completed after each cycle to ensure only the *g20* product was being measured and eliminate quantification of non-specific binding (Morrison et al. 1998, Matteson et al. 2011), as primer dimers were often evident at low copy numbers. Following amplification, a melting curve was read every 1° C from 40° to 95° C to check primer specificity and non-specific amplification. Negative controls were loaded with molecular biology grade water (Fisher Scientific) without DNA template. The detection limits for qPCR were previously determined by Matteson et al. as *ca*. 10 copies per reaction using this protocol (Matteson et al. 2013).

Flow cytometry and chlorophyll measurements

Flow cytometry and chlorophyll measurements were all performed by Dr. Zackary Johnson's group. Phytoplankton were enumerated using a FACSCalibur flow cytometer (Becton Dickinson) and cyanobacterial and eukaryotic phytoplankton populations were characterized as previously described (Johnson et al. 2010). Briefly, cells were excited with a 488 nm laser (15 mW Ar) and inelastic forward (<15°) scatter, inelastic side (90°) scatter (SSC), green (530 ± 30 nm) fluorescence, orange fluorescence (585 ± 42 nm), and red fluorescence (> 670 nm) emissions were measured. Population geometric mean properties (scatter and fluorescence) were

normalized to 1.0 µm yellow-green polystyrene beads (Polysciences, Warrington, PA) and typically have excellent reproducibility (5-10% CV) (Lin et al. 2013). To quantify heterotrophic bacteria, the samples were stained with SYBR Green-I (Molecular Probes Inc.) (Marie et al. 1997) and *Prochlorococcus* abundance was subtracted from the total bacterial population.

Chlorophyll concentrations were measured by filtering 100 mL of seawater sample onto a 22 µm, 2 µm or 20 µm pore size polycarbonate filter using a gentle vacuum (<100 mm Hg) and extracting in 100% MeOH at -20°C in the dark for >24 h (Holmhansen & Riemann 1978). Fluorescence was measured using a Turner Designs 10-AU fluorometer calibrated against a solid chlorophyll standard (Ritchie 2006) following Welschmeyer (1994).

Epifluorescence microscopy

Total viral abundances were determined from flash frozen (liquid N_2) samples fixed with 0.5% (v/v) glutaraldehyde and stored at -80° C. The protocol for obtaining total virus counts was followed as detailed in Ortmann and Suttle (2009). All reagents for epifluorescence microscopy were filtered with 0.02 µm pore size Anotop Plus syringe filters (Whatman®) to remove any viral particles. Samples were thawed on ice and diluted with filtered A+ media. Each diluted sample was vacuum filtrated onto a 0.02 µm pore size Anodisc™ filter (Whatman®). Filters were stained in the dark with 1:4000 diluted SYBR green (Lonza, Rockland, ME). Once dried, the filters were placed on slides fixed with antifade made from 50:50 PBS/glycerol and 0.1% *p*-phenylenediamine. Slides were either counted immediately or frozen at -20° C until later (two days maximum storage time). Each slide was thawed only 1 time before counting. Slides were

counted on a Leica DM5500 B at 1250 times magnification under blue excitation (λ_{Ex}, 440 to 480 nm; λ_{Em}, 527 to 530 nm) (Leica Microsystems, Wetzlar, Germany). At least 20 independent fields or 200 VLP were counted for each slide. The number of VLPs mL^{-1} (*Vt*) were calculated using the following equation (Ortmann & Suttle 2009):

$$Vt = \frac{Vc}{Fc} * \frac{At/Af}{S}$$

Where *Vc* = total number of VLPs counted per slide, *Fc* = total number of fields counted per slide, *At* = surface area of the filter (μm^2), *Af* = area of each field (μm^2), and *S* = volume of sample filtered (mL).

Virus-host contact rates and cell lysis estimates

Contact rates for the total virus community and the cyanomyoviral population (using *g20* abundance as a proxy) to heterotrophic bacteria and cyanobacteria (*Synechococcus*, and *Prochlorococcus*) were calculated according to the Murray and Jackson equation (1992), and as detailed in (Matteson et al. 2013):

$$\text{contacts } mL^{-1}\ day^{-1} = (2 \cdot S \cdot \pi \cdot \omega \cdot D_v) \cdot VB$$

Where VB = virus particles mL^{-1} x bacterial cells mL^{-1}. A diameter (ω) of 0.45 x 10^{-4} cm was used for heterotrophic bacteria (Lee & Fuhrman 1987), while a diameter of 1.0 x 10^{-4} cm was used for *Synechococcus* (Waterbury et al. 1986) and 0.5 x 10^{-4} cm for *Prochlorococcus* (Morel et al. 1993). Diffusivity of virus particles (*Dv*) was assumed to be 3.456 x 10^{-3} cm^2 day^{-1} as in Murray and Jackson (1992). A Sherwood number (*S*) of 1.06 was used since the population was assumed to be ~10% motile (Wilhelm et al. 1998). This number was then divided by the size

of the standing stock population in cells mL^{-1} to derive the number of contacts $cell^{-1}$ day^{-1}. Though the motile population would make up a smaller proportion of the combined *Synechococcus* and *Prochlorococcus* populations, the same Sherwood number was used to simplify calculations.

To estimate the rate at which *Synechococcus* and *Prochlorococcus* cells would need to be lysed to support the observed cyanophage population, a conservative decay rate of 0.5 day^{-1} and a previously determined burst size of 81 viruses per *Synechococcus* cell lysed (Garza & Suttle 1998) or 40 viruses per *Prochlorococcus* cell lysed. The combined cyanobacterial population inferred mortality rate estimated used a burst size of 81 viruses per cell to simplify calculations. Estimates of cells lysed day^{-1} were then divided by the estimated abundances of *Synechococcus* cells mL^{-1} to approximate the percentage of the standing population lysed to support observed cyanomyoviral abundances. All cyanobacteria lysed in the Pacific Ocean were estimated from surface abundances since decay rates have not been determined for the other depths sampled in this study.

Statistical analyses

Threshold cycle (C_t) calculations for each qPCR assay were completed using the MJ OPTICON Monitor Analysis software (ver. 3.1) with the Global Minimum setting. The threshold for all reactions was manually adjusted to obtain standard curves with the highest correlation coefficient (r^2). Standard curves (log gene copy number vs. C_t) for each qPCR assay were used to determine total gene copies in the samples. Wells with amplification efficiency under 50% were excluded from analysis. The relationships between biological parameters and *g20* gene copies were determined on untransformed abundances using R (ver. 0.97.314). Pearson and

Spearman correlations were determined using the corr.test function in the psych package (ver. 1.3.2). Other packages in R (such as ggplot2 [ver. 0.9.3], reshape [ver. 1.2.2], and plyr [ver. 1.2.12]) were used in combination with Sigmaplot (ver. 10) to visualize and transform data for analysis.

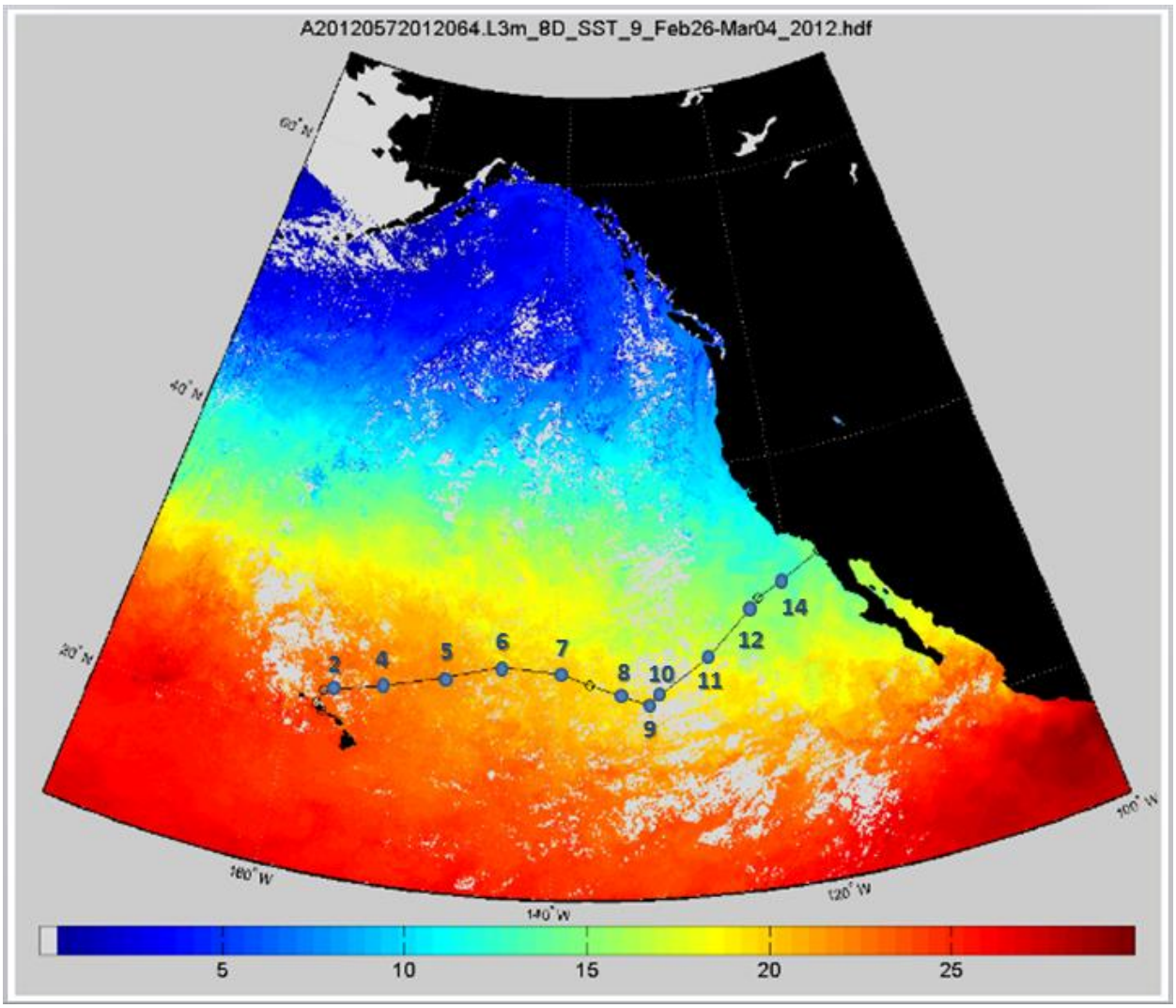

Figure 1. POWOW 1 cruise track satellite image. Points indicate sampling sites, and colors show the surface temperature in degrees Celsius. Image taken by NASA Aqua MODIS with cruise track and stations overlaid, February 26-March 4, 2012.

IV. RESULTS

Global trends across the cruise track

Environmental variation across the transect

Temperatures across all depths and stations ranged between 7.4° and 23.4° C (Fig. 2A). Predictably, higher temperatures were recorded in surface waters with progressively lower ones down through the water column. The lowest temperatures were recorded at the 300 m depths, as they fell below the thermocline for the entirety of the cruise. Surface temperatures ranged between 13.5° and 23.4° C. Salinity ranged between 25.04 and 35.43 psu (Fig. 2D). Recorded pH levels ranged between 7.66 and 8.10 (Fig. 3A). Temperature, pH, and salinity co-varied and decreased steadily over the cruise track from Hawaii to California.

Fluorescence remained below 1.5 FU (fluorescence units) for most of the transect, but reached levels as high as 34.13 FU at the last station (Fig. 2B). Dissolved oxygen was distributed somewhat evenly throughout the water column for the first several stations, and hovered around ~210 μmol Kg^{-1} for most of the transect (Fig. 2C). The last station, however, displayed more oxygen stratification than all the previous ones, with oxygen concentrations as low as 0.358 μmol Kg^{-1} at 300 m and as high as 253.55 μmol Kg^{-1} at the surface. Silicate concentrations ranged between 0.76 μM and 1.68 μM over most of the transect, steadily increasing from Hawaii to California until increasing sharply to their maximum concentration of 18.53 μM at 100 m in the last station (Fig. 3B). Phosphate concentrations were at their highest levels in coastal waters and lowest at pelagic stations, with concentrations ranging from undetectable to 1.27 μM (Fig. 3G). Nitrite concentrations were mostly recorded at values below the nominal detection limit but

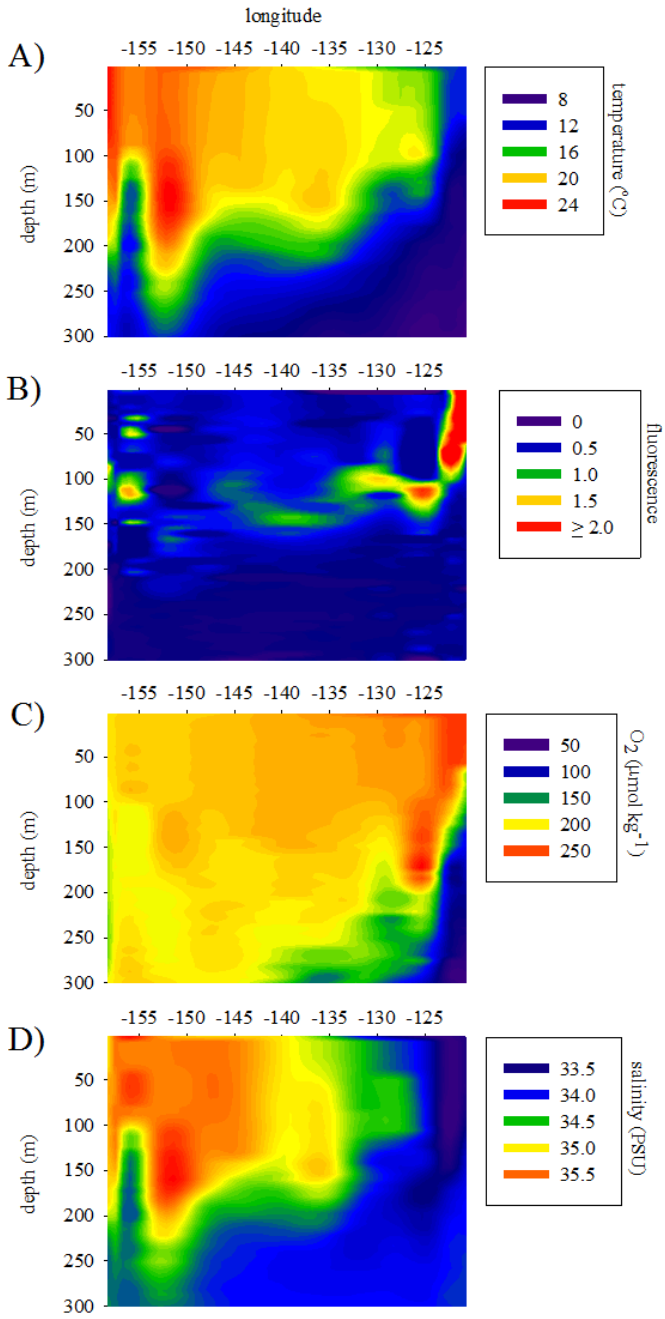

Figure 2. Environmental variation over the transect. Measurements were recorded every 1 m throughout the water column by a CTD mounted on the sampling rosette. The y-axis signifies the depth at which each measurement was taken, while the x-axis represents the position on the transect in longitude (degrees east). **(A)** Temperature in °C. **(B)** Fluorescence. **(C)** Dissolved oxygen, in µmol Kg^{-1}. **(D)** Salinity, in PSU.

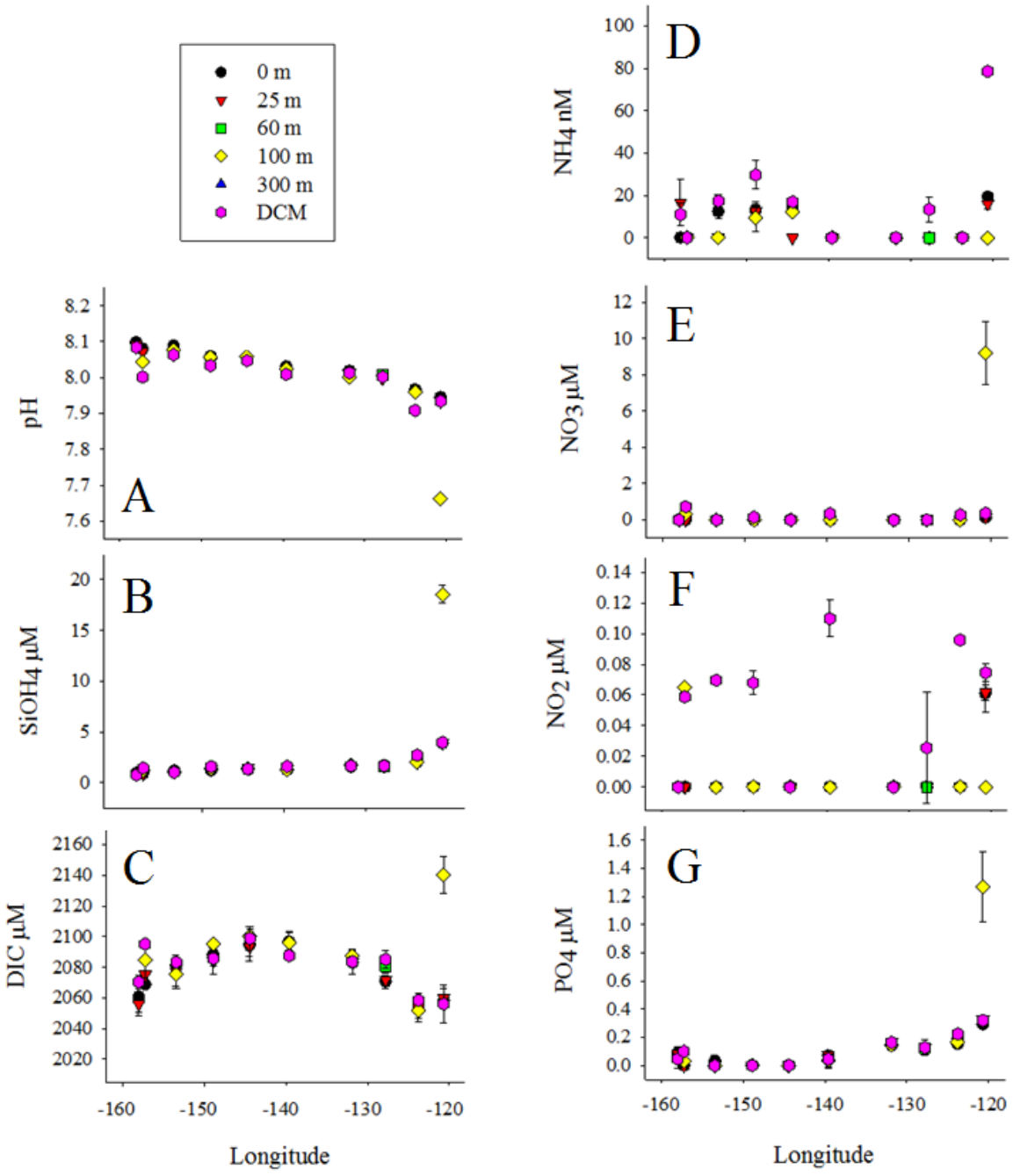

Figure 3. Variation in nutrient concentrations and acidity across the transect. Note that the y-axis scales are different for each plot. The x-axis corresponds to the longitude at which the sample was collected in degrees east. **(A)** pH. **(B)** Silicate concentrations, in µM. **(C)** Dissolved inorganic carbon concentrations, in µM. **(D)** Ammonia concentrations, in nM. **(E)** Nitrate concentrations, in µM. **(F)** Nitrite concentrations, in µM. **(G)** Phosphate concentrations, in µM.

had a maximum concentration of 0.11 μM, which was found at the DCM of an oligotrophic station (Fig. 3F). Ammonia concentrations were below detection limits for all depths at stations 8, 10, and 12, but they were also commonly found at levels between ~10 nM and ~30 nM across the transect (Fig. 3D). Some of the highest ammonia and nitrite concentrations occurred at the DCM depth at oligotrophic stations, but the highest overall ammonia concentration was found at the DCM of the final station (~79 nM). Nitrate concentrations, for the most part, remained at levels below the nominal detection limit over the entirety of the cruise with a few exceptions at coastal stations (max = 9.19 μM) (Fig. 3E). Generally, DIC concentrations increased with increasing distance from shore, though the maximum concentration was recorded at the coastal transition zone near the California coast (min = 2052 μM, max = 2140 μM) (Fig. 3C).

Biotic variation across the transect

Throughout the water column, total chlorophyll α (<0.22 μm) concentrations were highest at the DCM (as would be expected, since the DCM was determined to be the depth with maximum *in situ* fluorescence values) (min=0.023 μg L^{-1}, max=0.692 μg L^{-1}), with the exceptions of the surface at station 8 (longitude: 139.60 °E) and at 25 m at station 14 (longitude: -120.70 °E (Fig. 4E). To explain some of this disparity, it must be noted that at station 8, the DCM was sampled at 142 m, though the true DCM was at ~138 m. Chlorophyll α concentrations across the transect ranged between undetectable and 0.065 μg L^{-1} in the >20 μm fraction (Fig. 4F), and 0.005 μg L^{-1} and 0.271 μg L^{-1} in the >2 μm fraction (Fig. 4G). Both size fractionated chlorophyll concentrations were generally higher at coastal stations and decreased further from shore. The abundance of heterotrophic bacteria mL^{-1} varied throughout the water column, but was usually

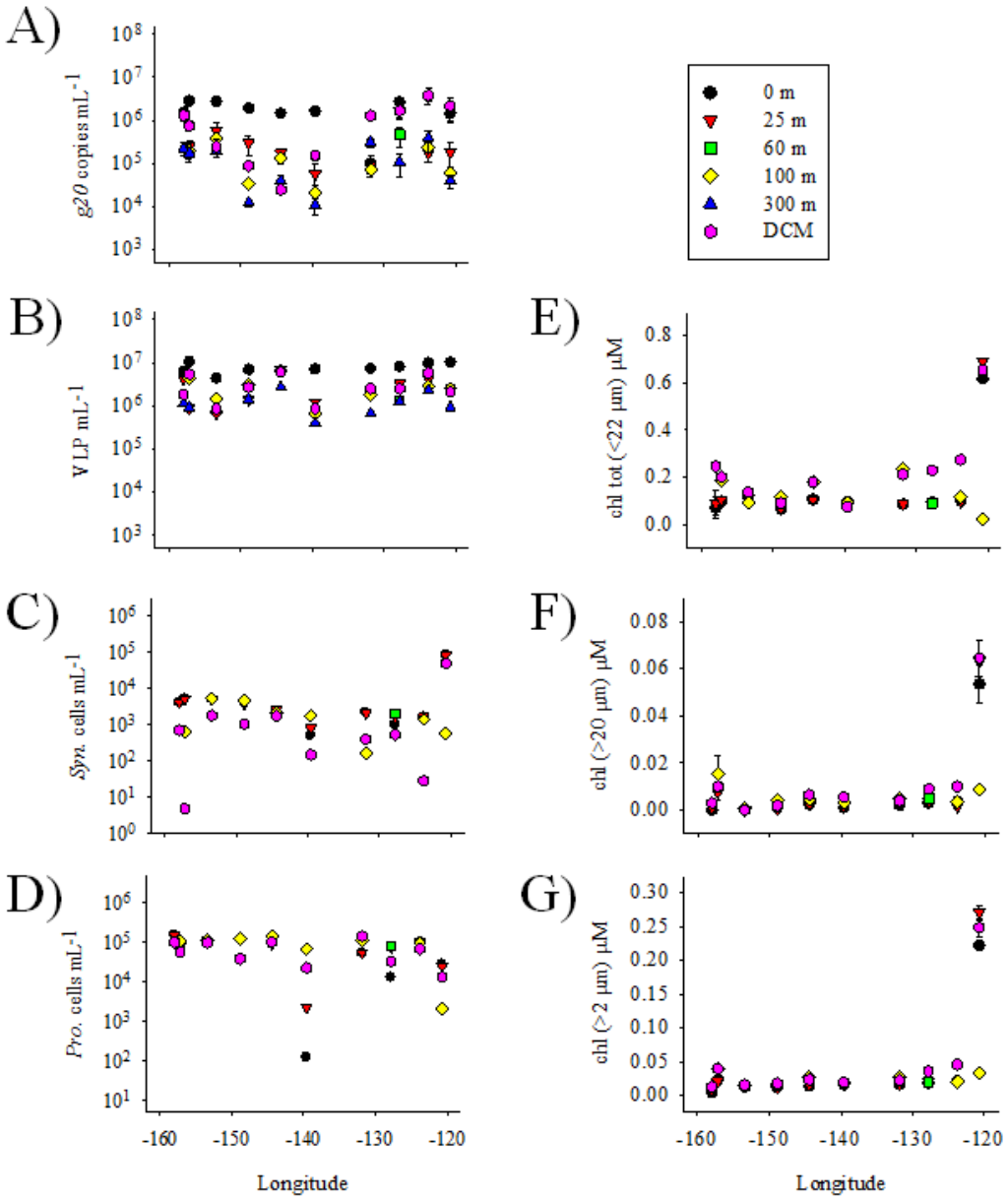

Figure 4. Biotic variation over the cruise transect. Note the different scales on each y-axis. The x-axis represents the longitude at which each sample was collected (in degrees east). Each shape and color corresponds to a different depth, as defined in the legend. Though measurements for additional depths were collected for the cyanobacterial counts and chlorophyll concentrations, only depths where cyanomyoviral counts were also taken are shown here for ease of comparison. **(A)** Cyanomyoviral abundance in *g20* copies mL^{-1}. **(B)** total viral density in VLP mL^{-1}. **(C)** *Synechococcus* density in cells mL^{-1}. **(D)** *Prochlorococcus* density in cells mL^{-1}. **(E)** total chlorophyll α concentration in µg L^{-1}. **(F)** Size fractionated chlorophyll α concentration in the >20 µm portion µg L^{-1}. **(G)** Size fractionated chlorophyll α concentration in the >2 µm portion µg L^{-1}. Error bars represent the standard deviation (SD) for A, E, F, and G. Where error bars are not visible, they do not exceed the width of the symbol.

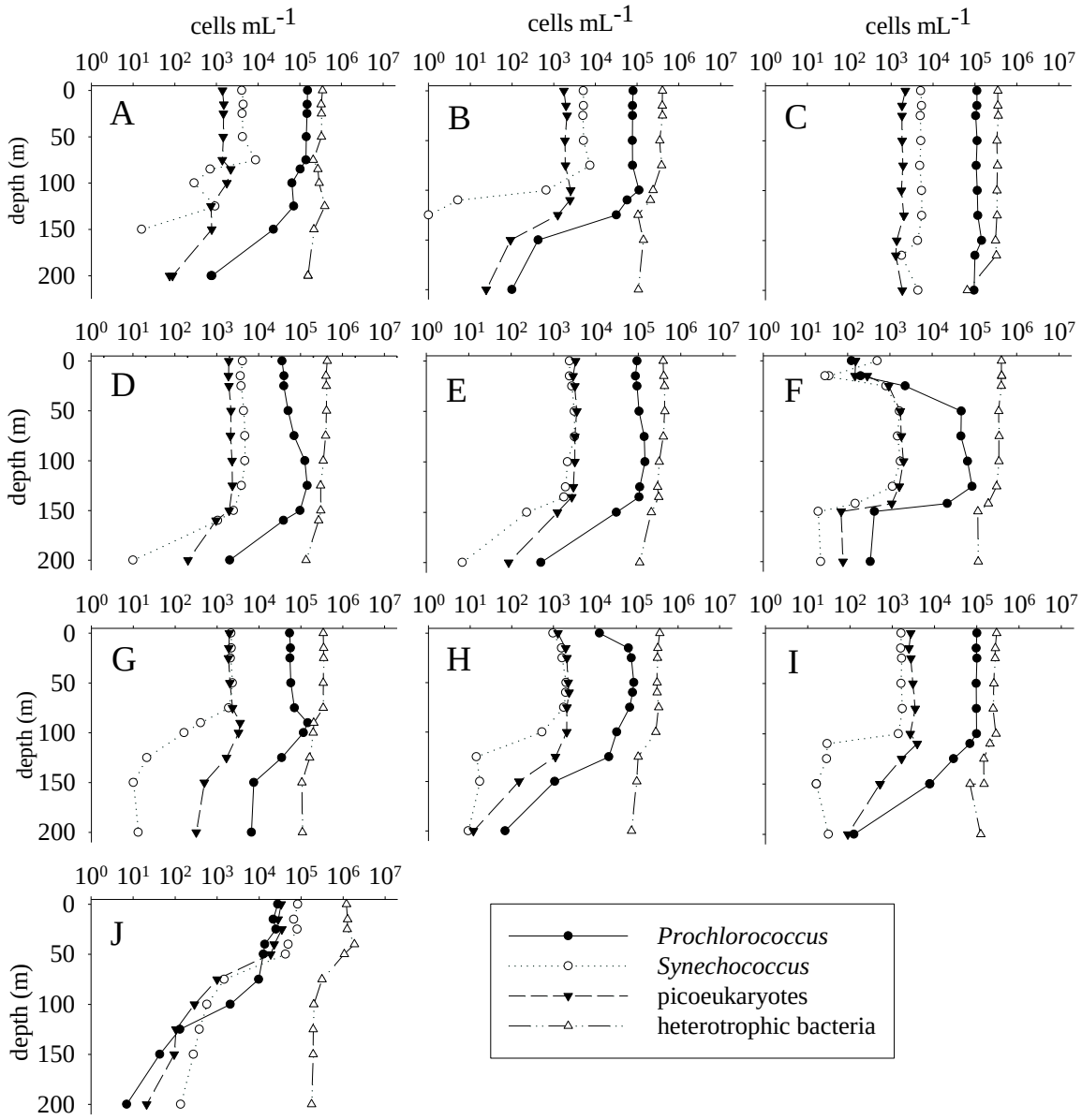

Figure 5. Bacterial distribution throughout the water column for each station. Each graph corresponds to the following stations and longitudes: **(A)** station 2, -158° E; **(B)** station 4, -157.21° E; **(C)** station 5, -153.43° E; **(D)** station 6, -148.89° E; **(E)** station 7, -144.41° E, **(F)** station 8, -139.60° E, **(G)** station 10, -131.85° E, **(H)** station 11, -127.80° E, **(I)** station 12, -123.78° E, **(J)** station 14, -120.70° E. The legend shows which line and symbol style corresponds to each bacterial count.

lowest at the DCM and highest near the surface (Fig. 5). Over the cruise, the number of heterotrophic bacteria hovered around ~10^5 cells mL^{-1} until the last station, where there was an abrupt spike in abundance to ~10^6 cells mL^{-1}. The number of *Prochlorococcus* cells ranged between ~10^3 and ~10^5 cells mL^{-1} and decreased gradually over the transect with the lowest abundances recorded at the last station (Fig. 4D, Fig. 5). *Synechococcus* abundances ranged between 5 and ~10^3 cells mL^{-1} over most of the transect and throughout the water column, but increased suddenly to ~10^4 cells mL^{-1} at the last station (Fig. 4C, Fig. 5). These picocyanobacterial abundances across the entire transect are within the range previously reported for the ALOHA (A Long-term Oligotrophic Habitat Assessment) station (*Prochlorococcus* max. ~2 x 10^5, *Synechococcus* max. ~2 x 10^3) (Campbell & Vaulot 1993). The *Synechococcus* and *Prochlorococcus* abundances are also similar to ones reported for the Southern Pacific Ocean and the Sargasso Sea, respectively (Matteson et al. 2013).

Total viral abundance ranged between ~10^5 and ~10^7 VLP mL^{-1} amongst all depths sampled (Fig. 4B). At the surface, viral density appeared to increase from station 2 (longitude: -158.00 °E) to station 14 (longitude: 120.70 °E), with the exception of the anomalously high abundance at station 4 (longitude: -157.21 °E). Viral abundances at 300 m were low compared to the other depths, though some stations had low abundances at other depths as well. Cyanomyoviral abundances (using *g20* copies mL^{-1} as a proxy for number of phages mL^{-1}) ranged between ~10^4 and ~10^6 phages mL^{-1} across the transect (Fig. 4A). Overall, the number of cyanomyoviruses was highest in the upper mixed layer and lowest at 300 m, with higher abundances recorded at coastal or coastal transition stations. Generally, cyanomyoviruses

outnumbered *Synechococcus* cells by around 3 orders of magnitude and *Prochlorococcus* by 1-3 orders of magnitude throughout the transect.

Coastal transition zone at station 14

Station 14, which was in the coastal transition zone off the coast of California, was characterized by sharp increases in the concentrations of phosphate, nitrate, and DIC (all at 100 m) and ammonium (DCM, 40 m), as well as significant decreases in pH and temperature (100 m) and salinity (DCM, 40 m) at certain depths. This station also displayed abrupt increases in eukaryotic phytoplankton abundance, *Synechococcus* abundance, and all chlorophyll concentrations (all depths except 100 m and 300 m), and a sharp decrease in *Prochlorococcus* abundance. For all previous stations, the upper mixed layer was ~5-6 °C warmer than the 300 m depth, however, there was only a 2.7 °C difference between 100 m and 300 m at station 14 (longitude: -120.70 °E). The lack of temperature variation throughout the water column in this area suggests that this is the site of deep water upwelling, thus explaining the increases in nutrients and phytoplankton abundance. For all previous stations, the oxygen ranged between 82.698 and 253.547 μmol O_2 Kg^{-1} throughout the water column. However, the oxygen concentrations for the DCM and 300 m depths at station 14 were markedly lower than previous stations, with measurements at 3.0317 μmol O_2 Kg^{-1} and 0.358 μmol O_2 Kg^{-1}, respectively. Taking into account the abrupt increases in nutrient concentrations, biotic variables, and wide fluctuations in oxygenation indicate that station 14 is much more productive than any of the other stations sampled.

Correlations and calculated parameters

Correlational analyses

Since assumptions of normality were not met for all the collected data, Spearman correlation analyses were performed instead of the more commonly used Pearson correlation analyses. Spearman correlation analyses revealed many significant monotonic (rank-order) relationships between biological and environmental parameters, as shown in Table 2 and Figure 6. Significant positive correlations were found between cyanomyophage abundance and DIC (Fig. 7B), cyanomyophage abundance and total viral density (Fig. 7A), cyanomyophage abundance and depth, and total viral density and depth (Table 3).

Contact rates, inferred mortality, and % cyanomyophage

Inferred mortality rates of the *Synechococcus* standing stock in surface waters were incredibly high across the transect, ranging between 11% and 2037% (Table 3). Only two stations reported mortality rates below 100% of the *Synechococcus* standing stock. Previously, the maximum observed percentage of *Synechococcus* standing stock required to be lysed to maintain the observed cyanomyoviral population was only 46% (Matteson et al., 2013). The inferred mortality rates for *Prochlorococcus* ranged between 2% and 16,768% across the transect, however, only two stations had rates which exceeded 100% (station 8 with 16,768% and station 11, with 258%) (Table 3). Excluding the stations with rates higher than 100%, the maximum inferred mortality rate for *Prochlorococcus* was 67%. The inferred mortality rates reported in this study appear to be driven by the high cyanomyoviral abundances along with occasional crashes in cyanobacterial abundance, such as the one observed at station 8 where both *Synechococcus* and *Prochlorococcus* abundances dipped to ~10^2 cells mL^{-1} (Fig. 5). Contact

rates for total viral abundance versus cell counts ranged between 10.24 and 24.4 contacts cell^{-1} day^{-1} for *Synechococcus*, between 5.12 and 12.2 contacts cell^{-1} day^{-1} for *Prochlorococcus*, and between 4.61 and 10.98 contacts cell^{-1} day^{-1} for heterotrophic bacteria (Table 3). The contact rates for *g20* copies versus bacterial counts were between 0.24 and 8.4 contacts cell^{-1} day^{-1} for *Synechococcus*, between 0.12 and 4.2 contacts cell^{-1} day^{-1} for *Prochlorococcus*, and between 0.11 and 3.78 contacts cell^{-1} day^{-1} for heterotrophic bacteria (Table 3). Cyanomyoviruses throughout the water column were estimated to account for anywhere between 0.8% and 101% of the total viral population (Fig. 7). These percentages are much higher than those previously observed (Matteson et al., 2013). Cyanomyoviral abundance for sample ID 2 (station 2, 25 m) was excluded from analysis since all replicates had an amplification efficiency of ~20-30%, which was much lower than the efficiency cut-off of 50%. Cyanomyoviral abundances were also not obtained for sample ID 3 because the cryovial was lost during processing (CTD 2, 100 m). Over 800 cyanophage isolates were obtained through plaque plating, but it is currently unknown how many are unique phage, and *g20* screenings have not yet been performed. Underway data is supplied in the Appendix (Fig. 9, Fig. 10), but is not discussed in detail since it cannot be compared to the other data collected here.

Table 2. Spearman correlation matrix of relationship between *g20* copies and environmental parameters on the POWOW1 cruise.

Parameter		
Viral density	P = **0.014**	r_s = **0.393**
Heterotrophic bacteria	P = 0.255	r_s = 0.189
Picoeukaryotes	P = 0.494	r_s = 0.114
Prochlorococcus	P = 0.702	r_s = -0.064
Synechococcus	P = 0.546	r_s = 0.101
Chl (>2 μm)	P = 0.857	r_s = -0.030
Chl (>20 μm)	P = 0.948	r_s = 0.011
Total chl (<22 μm)	P = 0.292	r_s = 0.176
Dissolved O_2	P = 0.891	r_s = 0.023
pH	P = 0.889	r_s = 0.023
Salinity	P = 0.623	r_s = -0.082
Temperature	P = 0.904	r_s = 0.020
Depth	P = **0.003**	r_s = **-0.471**
DIC	P < **0.001**	r_s = **-0.522**
NH_4	P = 0.770	r_s = 0.049
NO_2	P = 0.526	r_s = 0.106
NO_3	P = 0.895	r_s = -0.022
PO_4	P = 0.491	r_s = 0.115

P, unadjusted P-values

r_s, Spearman correlation coefficient

Those significantly correlated ($P < 0.05$) are shown in bold face

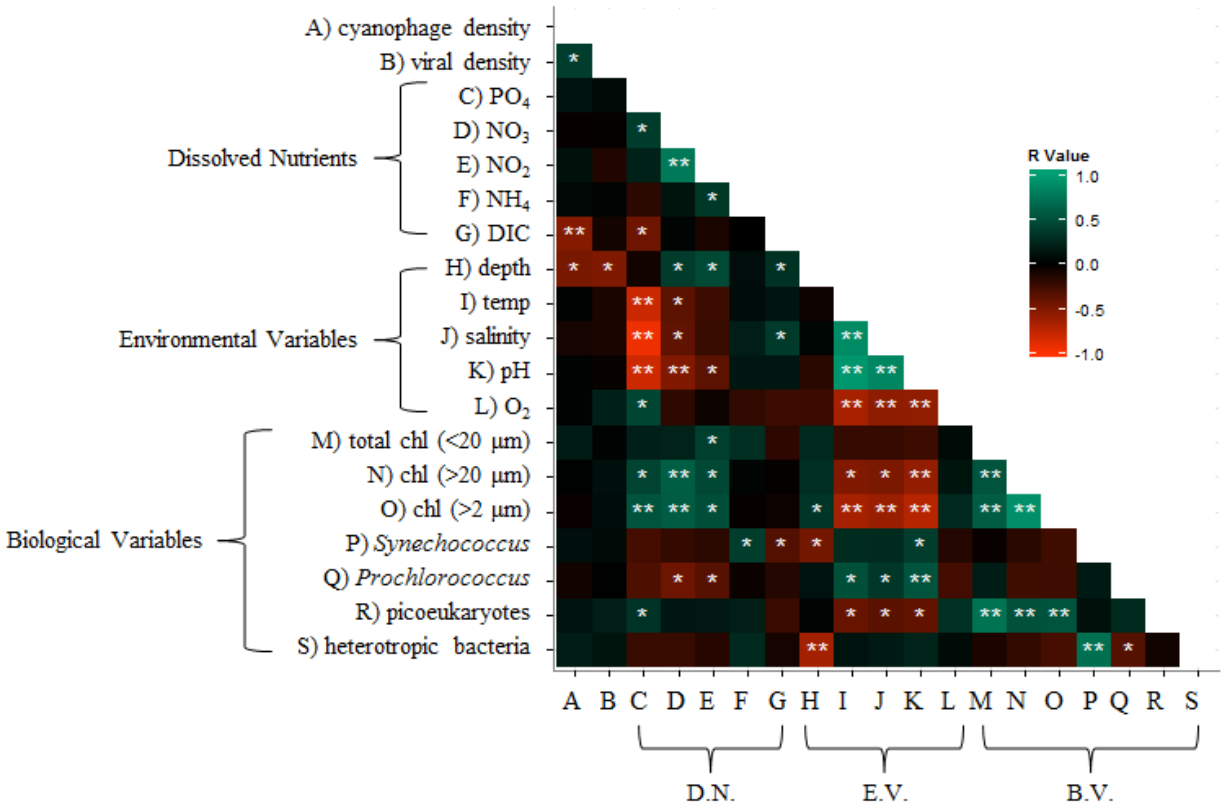

Figure 6. Spearman correlation heat map of all biological and environmental parameters for the upper mixed layer. Samples at 300 m were excluded from this analysis, as it explores the relationships for the upper mixed layers only. The colored squares indicate the strength and direction (R value) of each correlation, with green implicating a positive correlation and red a negative correlation. Stars indicate the significance level, where "*" designates a p-value ≤0.05, and "**" a p-value ≤0.001. Variables are grouped based on their category. A and B are both viral parameters, though they are not designated on the chart.

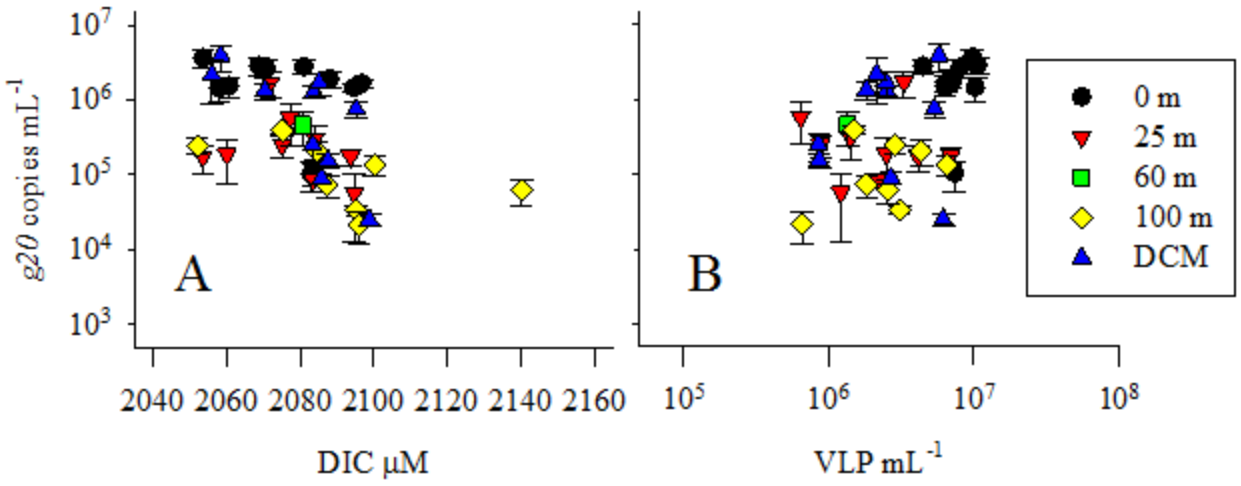

Figure 7. Significant correlations between cyanomyoviral abundance and other variables.
(A) Cyanomyoviral abundance (in *g20* copies mL^{-1}) vs. DIC (in µM) ($P < 0.001$, $r_s = -0.5215$).
(B) Cyanomyoviral abundance vs. viral density (in VLP mL^{-1}) ($P = 0.0146$, $r_s = 0.393$).

Table 3. Contact rates and inferred mortality in the surface waters of the North Pacific Ocean. The specific contact rates for total viral counts and putative cyanomyoviral abundances are shown in columns 3-8. The 9th and 10th columns show the number of *Syn* or *Pro* cells mL^{-1} day^{-1} that need to be lysed in order to maintain the observed cyanomyoviral density. These numbers are calculated via the Murray and Jackson equation (1992) discussed in the Methods, assuming an average burst size of 81 for *Synechococcus*, 40 for *Prochlorococcus*, and 81 for *Syn.* + *Pro*. The % lysed column shows the percentage of *Syn.* and *Pro.* standing stock that would need to be lysed to replace 50% of the observed cyanomyoviral abundance.

		Specific contact rate ($cell^{-1}$ day^{-1})										
		Total viruses vs.			*g20* genes vs.			*Syn.* lysed	*Pro.* lysed			
Stn.	Longitude	*Syn.*	*Pro.*	HB	*Syn*	*Pro*	HB	(cells mL^{-1} day^{-1})	(cells mL^{-1} day^{-1})	*Syn.* % lysed	*Pro.* % lysed	*Pro.+Syn. % lysed*
*2	-158	14.52	7.26	6.54	3.54	1.77	1.60	9506	19250	234%	13%	6%
4	-157.21	24.40	12.20	10.98	6.58	3.29	2.96	17654	35750	344%	45%	21%
5	-153.42	10.24	5.12	4.61	6.40	3.20	2.88	17160	34750	338%	31%	15%
6	-148.89	15.84	7.92	7.13	4.44	2.22	2.00	11914	24125	292%	67%	30%
7	-144.41	14.78	7.39	6.65	3.36	1.68	1.51	9012	18250	377%	20%	9%
8	-139.60	16.09	8.04	7.24	3.80	1.90	1.71	10185	20625	2037%	16768%	1635%
10	-131.85	16.85	8.42	7.58	0.24	0.12	0.11	636	1287.5	30%	2%	1%
11	-127.81	18.62	9.31	8.38	6.15	3.07	2.77	16481	33375	1685%	258%	118%
12	-123.78	22.60	11.30	10.17	8.40	4.20	3.78	22531	45625	1395%	45%	22%
14	-120.70	23.48	11.74	10.57	3.31	1.66	1.49	8889	18000	11%	65%	8%

Syn. = Synechococcus

Pro. = Prochlorococcus

HB = heterotrophic bacteria

Stn. = station number

* = station ALOHA

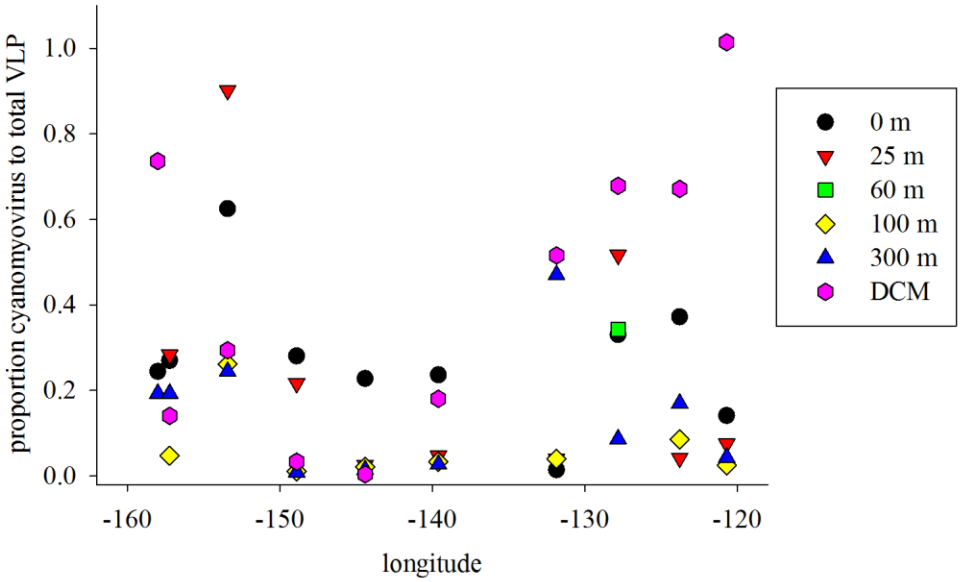

Figure 8. Proportion of cyanomyovirus to total viral counts. The x-axis represents the proportion of putative cyanomyoviruses to total viral counts, while the y-axis represents the longitude at which the sample was collected in degrees east. The legend indicates the depth at which each sample was collected.

V. DISCUSSION

To this day, only three studies have focused on the quantification of cyanomyoviruses in aquatic environments (Sandaa & Larsen 2006, Matteson et al. 2011, Matteson et al. 2013). One of these was performed in a freshwater lake (Matteson et al. 2011), and none of which sampled depths below 25 m. Here, we sampled depth profiles extending from the surface to 300 m, and used qPCR to quantify cyanomyophages across an environmental gradient in the Pacific Ocean. We discuss the data generated through this expansive study to help address the dearth in understanding of how cyanomyoviral abundance is constrained in different environments.

Correlations between cyanophage and environmental and biotic parameters

Though evidence exists to support the idea that phosphate is an influential factor on cyanophage proliferation (Wilson et al. 1996, Zeng & Chisholm 2012), our study did not reveal any significant relationships between cyanomyophage abundance and dissolved phosphate concentrations in the Pacific Ocean. We also did not find any significant relationships between viral or cyanomyoviral abundance and temperature. Instead, cyanomyoviral abundance correlated only with depth (Fig. 6, Table 2), total viral density (Fig. 7A), and DIC (Fig. 7B). Total viral density also correlated negatively with depth (Table 2, Fig. 6), which is consistent with other studies (Danovaro et al., 2011). It is likely that the negative correlation between DIC and putative cyanomyoviral abundance is not indicative of any interaction between the two variables. Instead, it may indicate a relationship between cyanophage abundance and distance from shore, as has been observed previously (Suttle & Chan 1994). However, one study found an inverse correlation between DIC concentration and bacterial productivity in the Indian Ocean, suggesting that lower DIC concentrations may serve as an indicator of higher bacterial

productivity (Ishii et al. 1998). Indeed, the DIC concentrations in this study were lowest near coastal areas, which are normally characterized by higher productivity, and indicates there was increased CO_2 consumption by phototrophs. However, cyanomyoviral abundance did not correlate with any of the chlorophyll α fractions, which are very indirect measures of primary productivity (Behrenfeld & Falkowski 1997).

Cyanomyoviral distribution

Cyanomyophage abundances ranged between 10^4 and 10^6 cyanomyophages mL^{-1} for most of the transect, then reached their maximum abundance of 3.86 x 10^6 phages mL^{-1} at station 14 (Fig. 4A). These maximum cyanophage abundances are similar to ones reported for Lake Erie (Matteson et al. 2011), but are higher than those recorded in the South Pacific by one order of magnitude (Matteson et al. 2013) and at the Norwegian coast by roughly three orders of magnitude (Sandaa & Larsen 2006). They are also higher than the cyanophage abundances found in the Gulf of Mexico (~10^5 cyanophage mL^{-1}) (Garza & Suttle 1998), which were determined through most probable number (MPN) assays using *Synechococcus* strains as hosts, and therefore assumed to be underestimates of cyanophage density. In this study, putative cyanomyoviruses were distributed through the water column in a depth dependent manner, with higher densities at the surface (between ~10^5 and ~10^6 *g20* copies mL^{-1}) and decreasing abundances lower down (Fig. 4A). However, at the 300 m depth, cyanomyoviral densities occurred in high abundances between ~10^4 and ~10^5 *g20* copies mL^{-1}, which is comparable to the numbers observed in the surface waters of the Sargasso Sea (Matteson et al. 2013). Generally, *Prochlorococcus* and *Synechococcus* abundances were higher in the upper mixed layer, then dropped abruptly between 100 m and 150 m (Fig. 5), except for station 5, which had

almost uniform abundances for all cell counts down to 200 m (Fig. 5C). Though cyanobacterial counts were only quantified in the upper mixed layer and down to 200 m, it may be safely assumed that 300 m depths contained lower cyanobacterial abundances than those seen at 200 m. Because of this, the high density of putative cyanomyoviruses at 300 m is unexpected, since there are few hosts for them to infect, and productivity at these depths should be low (Morel et al. 1996). It is likely that these cyanomyoviruses are largely composed of phage particles attached to marine snow (Weinbauer et al. 2011) since qPCR targets both infectious and noninfectious cyanomyophage. However, *Prochlorococcus* has been detected at depths below 150 m at abundances of around 10^3 cells mL^{-1} (Flombaum et al. 2013), and infectious phages have been known to persist in sediments (Hargreaves et al. 2013), so it is possible that there could be a small infectious population of cyanomyoviruses at these depths.

Previously, the percentage of cyanomyophage to the total viral community has been recorded at levels up to ~25.5% (Matteson et al. 2013), however, the percentages reported here ranged between 0.41% and 90.17%, with one sample at 101.4% (Fig. 8). Of these, the highest proportions of putative cyanophage occurred at the DCM (station 2, station 12, station 14), surface (station 5), 25 m (station 5), and 100 m (station 11) depths. Since it is highly unlikely that 100% of the viral community could be cyanomyophages (as was predicted at the DCM depth of station 14), there must be some alternative explanation. For example, most of the samples with high cyanophage percentages were characterized by lower total viral counts and higher cyanobacterial counts. It is also important to note that the qPCR approach can target viral genes inside host cells as well as within free phage particles, while epifluorescence microscopy allows the enumeration of only free viral particles with dsDNA genomes large enough to permit

adequate SYBR Green I staining for visualization (Suttle & Fuhrman 2010). The range of total viral abundances as quantified through epifluorescence microscopy were also around ten-fold lower throughout the cruise as compared to a previous study in the South Pacific (Matteson et al. 2013). Therefore, it is possible that a high proportion of the viral community were actively infecting the abundant hosts at the sampling site. This may be due to a high rate of lysogeny and/or pseudolysogeny in oligotrophic waters (Ortmann et al. 2002, Weinbauer 2004, Paul 2008). Whether or not cyanomyoviruses may have also been participating in pseudolysogeny is not yet known, since all cyanomyophages isolated to date have demonstrated lytic activity (Mann 2003). However, it is known that the closely related T4 virus is capable of pseudolysogeny under unfavorable host conditions (Los et al. 2003).

The low total viral abundances could also be explained by the idea that cyanophage infection may occur on a predictable diel cycle, where cyanophage infection and proliferation occurs during daylight hours, and cyanophage "hide out" within their hosts without lysing them during the night (Winter et al. 2004, Kimura et al. 2012). Since our sampling time was just before dawn (*c.* 5:30 am, local time), it is possible that we had a high rate of intracellular infection without as many free viral particles because cyanophage proliferation would not have occurred during the night, and free viral particles which were not able to successfully infect a host may have been removed from the system through grazing (Gonzalez & Suttle 1993). However, evidence suggests that cyanobacteria infected with phage may be preferentially grazed because of their high nutrient content (Evans & Wilson 2008), thus eliminating some proportion of actively infected cyanobacteria. In the future, it may be beneficial to assess the proportion of

total bacteria and cyanobacteria that are infected with phage at the time and location of sampling as well as quantifying cyanomyoviral and total viral density.

High cyanomyophage mediated inferred mortality rates

The Murray and Jackson equation was used to calculate the percentage of the *Synechococcus* standing stock which would need to be lysed to produce observed cyanomyoviral abundances (also known as the inferred mortality rate) (Murray & Jackson 1992). This inferred mortality rate is used to determine whether the observed cyanomyoviral abundances are within realistic ranges. In this study, inferred mortality rates for *Synechococcus* ranged between 11% and ~2000%, indicating that up to 20x the standing *Synechococcus* stock would need to be lysed to maintain the cyanomyoviral population (Table 3). These numbers are much higher than those previously reported for any environment, including the South Pacific, which had a maximum *Synechococcus* inferred mortality rate of ~46% (Matteson et al., 2013). In reality, cyanophage probably lyse a proportion of both *Synechococcus* and *Prochlorococcus* that cannot yet be calculated. To determine the proportion of *Prochlorococcus* cells that would need to be lysed to maintain these cyanomyoviral abundances, it is necessary to first figure out the average burst size for phage infected *Prochlorococcus* cells. This, unfortunately, has not yet been discerned, but evidence suggests that burst size can be predicted quite accurately when the host genome and phage genome sizes are known (Brown et al. 2006). Since the average *Prochlorococcus* genome is around half the size of *Synechococcus'* (~1.9 Mbp and ~4.7 Mbp, respectively) (Partensky et al. 1999, Brown et al. 2006), it may be that the burst size for *Prochlorococcus* is also half as large. Substituting a burst size of 40 phages cell^{-1} into the Murray and Jackson equation yields inferred mortality rates for *Prochlorococcus* which range between 2% and 67% for most stations,

but increase to 258% at station 11 and 16768% at station 8 (Table 3). When we calculate the mortality rate for the entire cyanobacterial population, we get more realistic numbers which range between 1% and 30% for most of the transect, and then spike to 118% at station 11 and 1635% at station 8 (Table 3). A caveat to this calculation is that it assumes the average burst size for the combined *Synechococcus* and *Prochlorococcus* population is 81 virus particles $cell^{-1}$, since it is impossible to determine what proportion of each are lysed by cyanomyoviruses. Regardless, the extremely high inferred mortality rates at stations 8 and 11 could be caused by a temporal disconnect between phage infection and cell lysis (Matteson et al. 2012). This may be true for station 8 especially, since both the *Pro.* and *Syn.* surface densities drop to ~10^2 cells mL^{-1}, which are the lowest surface abundances observed for either population across the transect (Fig. 5). These low abundances could signify the aftermath of a sizeable lysis or other destructive event from the previous day, such as photobleaching (Prezelin et al. 1987). These could also be the result of a flow cytometry error.

Hypotheses to explain high cyanomyoviral abundances compared to hosts

Our data have raised many questions about the origin of these high cyanomyoviral abundances observed across the transect and deep in the water column. To explain these phenomena, we propose the following hypotheses:

1. Plasmid supercoiling caused artificial inflation of *g20* abundance by altering standard curves.
2. The true decay rates or burst sizes in the North Pacific differed from the values used in the Murray and Jackson equation.

3. The CPS1 and CPS2 primers amplify non-cyanophage genes which were present across the transect.
4. These observations are real, but offset by the temporal nature of the phage-host relationship.

In some studies, it has been shown that supercoiled plasmid configuration may significantly increase abundance estimates in certain qPCR assays (Lin et al. 2011) but not others (Oldham & Duncan 2012). The assays which were affected by supercoiling produced much more accurate, and lower, abundance estimates when linear plasmid standards were used instead of circular ones (Lin et al. 2011). In each of our qPCR plates, we quantified triplicate samples containing a known number of S-PWM1 viral particles. In most plates, the estimated number of *g20* copies in the S-PWM1 wells was 1.5-2 times the abundance estimated through epifluorescence microscopy, with one plate producing an estimate ~9x higher, and 4 plates producing estimates that were somewhat lower than expected (data not shown). Though there was significant variation between each plate as far as S-PWM1 quantification, the standard deviations of replicate wells on each individual plate were within acceptable ranges. The variation inherent in this assay, as documented here and in Matteson et al. (2011 and 2013), may be due to the presence of different plasmid configurations in each standard aliquot. Therefore, it could be beneficial in the future to assess whether linearizing *g20* plasmid standards may produce more accurate cyanomyoviral abundance estimates.

It is almost certain that the actual burst sizes for phage infected cyanobacterial populations in the North Pacific differed from those we used in the Murray and Jackson equation. Burst sizes as high as ~250 virus particles cell^{-1} have been reported for cyanophage

infecting *Synechococcus* cells (Suttle & Chan 1994). However, these high burst sizes are generally seen in productive, coastal areas, and lower burst sizes around 20-25 viruses cell^{-1} are commonly observed in oligotrophic waters (Wommack & Colwell 2000). Therefore, though this hypothesis has a high likelihood of being falsified, it may not explain our observations.

These data may also be explained by the oft-touted criticism that the primers used in this study may amplify genes from unintended targets (Short & Suttle 2005, Wilhelm et al. 2006, Sullivan et al. 2008). However, these primers were recently verified with the De-MetaST-BLAST program (Gulvik et al. 2012) via BLASTing across the Global Ocean Survey data set (Williamson et al. 2008) so they should only amplify cyanomyoviral amplicons. Additionally, 9 qPCR amplicons from this study (sampled from station 11 at 25 m) were cloned and sequenced and each was subjected to a BLASTn search against the NCBI nucleotide library to see if there were any identifiable matches. Though the amplicons were too small to perform robust phylogenetic analysis, they were all the expected size (~165 bp) and returned highly similar hits to cultured and uncultured cyanomyoviral *g20* amplicons (data not shown). This provides more evidence against the hypothesis that these primers amplify non-cyanomyoviral targets.

As mentioned previously, evidence suggests that cyanophage may operate on a diel infection cycle (Kimura et al. 2012), and that the activity of the viral community may lag at least 24 hours behind that of their hosts (Matteson et al. 2012, Matteson et al. 2013). This could explain our observations of high cyanomyoviral abundances across the transect and resulting inferred mortality rates since the current standing population would not necessarily reflect the size of the population from which these phages originated. In fact, if the rate of production

outpaced that of removal, the cyanomyoviral abundances observed here may have resulted over several days of accumulation.

VI. CONCLUSIONS

Previously, most quantitative studies of cyanomyophage have been restricted to the upper mixed layer. This study collected quantitative biological and environmental data on a large spatial scale in the North Pacific Ocean, while also sampling down to 300 m. The high cyanomyoviral counts observed over the transect call the specificity of the qPCR assay used here into question, but may actually represent true abundances since no alternative gene target has been identified. If so, cyanomyoviruses may have larger impacts on ecological functioning than previously realized. We have suggested linearizing *g20* standard plasmids in future studies to combat possible overestimation of true abundances due to plasmid supercoiling. This study has also provided some evidence that temporal disconnects may hamper investigations of constraints on cyanomyoviral abundance, since cyanomyoviral abundances did not correlate significantly with either *Synechococcus* or *Prochlorococcus* populations. More Lagrangian style studies should be performed to discern the effects of diel cycles and temporal host-phage interactions on cyanomyoviral production in different marine environments.

LIST OF REFERENCES

Behrenfeld MJ, Falkowski PG (1997) Photosynthetic rates derived from satellite-based chlorophyll concentration. Limnology and Oceanography 42:1-20

Bergh O, Borsheim KY, Bratbak G, Heldal M (1989) High abundance of viruses found in aquatic environments. Nature 340:467-468

Bongiorni L, Magagnini M, Armeni M, Noble R, Danovaro R (2005) Viral production, decay rates, and life strategies along a trophic gradient in the North Adriatic Sea. Applied Environmental Microbiology 71:6644-6650

Borsheim KY (1993) Native marine bacteriophages. FEMS Microbiology Ecology 102:141-159

Bratbak G, Egge JK, Heldal M (1993a) Viral mortality of the marine alga *Emiliania huxleyi* (Haptophyceae) and termination of algal blooms. Marine Ecology Progress Series 93:39-48

Bratbak G, Heldal M, Naess A, Roeggen T (1993b) Viral impact on microbial communities. In R Guerrero and C Pedros-Alio. Trends in Microbial Ecology 299-302. Spanish Society for Microbiology, Barcelona

Bratbak G, Heldal M, Norland S, Thingstad TF (1990) Viruses as partners in spring bloom microbial trophodynamics. Applied Environmental Microbiology 56:1400-1405

Brown CM, Lawrence JE, Campbell DA (2006) Are phytoplankton population density maxima predictable through analysis of host and viral genomic DNA content? Journal of the Marine Biological Association of the United Kingdom 86:491-498

Brussaard CPD, Wilhelm SW, Thingstad F, Weinbauer MG, Bratbak G, Heldal M, Kimmance SA, Middelboe M, Nagasaki K, Paul JH, Schroeder DC, Suttle CA, Vaque D, Wommack KE (2008) Global-scale processes with a nanoscale drive: The role of marine viruses. ISME Journal 2:575-578

Campbell L, Vaulot D (1993) Photosynthetic picoplankton community structure in the subtropical North Pacific Ocean near Hawaii (station ALOHA). Deep-Sea Research Part I-Oceanographic Research Papers 40:2043-2060

Clokie MRJ, Shan JY, Bailey S, Jia Y, Krisch HM, West S, Mann NH (2006) Transcription of a 'photosynthetic' T4-type phage during infection of a marine cyanobacterium. Environmental Microbiology 8:827-835

Danovaro R, Corinaldesi C, Dell'Anno A, Fuhrman JA, Middelburg JJ, Noble RT, Suttle CA (2011) Marine viruses and global climate change. FEMS Microbiology Reviews 35:993-1034

Eppley RW, Renger EH, Venrick EL, Mullin MM (1973) Study of plankton dynamics and nutrient cycling in central gyre of North Pacific Ocean. Limnology and Oceanography 18:534-551

Evans C, Wilson WH (2008) Preferential grazing of *Oxyrrhis marina* on virus-infected *Emiliania huxleyi*. Limnology and Oceanography 53:2035-U2012

Flombaum P, Gallegos JL, Gordillo RA, Rincon J, Zabala LL, Jiao N, Karl DM, Li WKW, Lomas MW, Veneziano D, Vera CS, Vrugt JA, Martiny AC (2013) Present and future global distributions of the marine cyanobacteria *Prochlorococcus* and *Synechococcus*. Proceedings of the National Academy of Sciences of the United States of America 110:9824-9829

Fuller NJ, Wilson WH, Joint IR, Mann NH (1998) Occurrence of a sequence in marine cyanophages similar to that of T4 *g20* and its application to PCR-based detection and quantification techniques. Applied Environmental Microbiology 64:2051-2060

Garza DR, Suttle CA (1998) The effect of cyanophages on the mortality of *Synechococcus* spp. and selection for UV resistant viral communities. Microbial Ecology 36:281-292

Gonzalez JM, Suttle CA (1993) Grazing by marine nanoflagellates on viruses and virus-sized particles - ingestion and digestion. Marine Ecology-Progress Series 94:1-10

Gulvik CA, Effler TC, Wilhelm SW, Buchan A (2012) De-MetaST-BLAST: A tool for the validation of degenerate primer sets and data mining of publicly available metagenomes. PLOS One 7:e50362-e50362

Hargreaves KR, Anderson NJ, Clokie MRJ (2013) Recovery of viable cyanophages from the sediments of a eutrophic lake at decadal timescales. FEMS Microbiology Ecology 83:450-456

Holmes RM, Aminot A, Kerouel R, Hooker BA, Peterson BJ (1999) A simple and precise method for measuring ammonium in marine and freshwater ecosystems. Canadian Journal of Fisheries and Aquatic Sciences 56:1801-1808

Holmhansen O, Riemann B (1978) Chlorophyll *a* determination - improvements in methodology. Oikos 30:438-447

Huang SJ, Wang K, Jiao NZ, Chen F (2012) Genome sequences of siphoviruses infecting marine *Synechococcus* unveil a diverse cyanophage group and extensive phage-host genetic exchanges. Environmental Microbiology 14:540-558

Ishii M, Inoue HY, Matsueda H, Tanoue E (1998) Close coupling between seasonal biological production and dynamics of dissolved inorganic carbon in the Indian Ocean sector and the western Pacific Ocean sector of the Antarctic Ocean. Deep-Sea Research Part I-Oceanographic Research Papers 45:1187-1209

Johnson ZI, Shyam R, Ritchie AE, Mioni C, Lance VP, Murray JW, Zinser ER (2010) The effect of iron and light-limitation on phytoplankton communities of deep chlorophyll maxima of the western Pacific Ocean. Journal of Marine Research 68:283-308

Kibbe WA (2007) OligoCalc: An online oligonucleotide properties calculator. Nucleic Acids Research 35:W43-W46

Kimura S, Yoshida T, Hosoda N, Honda T, Kuno S, Kamiji R, Hashimoto R, Sako Y (2012) Diurnal infection patterns and impact of *Microcystis* cyanophages in a Japanese pond. Applied Environmental Microbiology 78:5805-5811

Labonte JM, Reid KE, Suttle CA (2009) Phylogenetic analysis indicates evolutionary diversity and environmental segregation of marine podovirus DNA polymerase gene sequences. Applied Environmental Microbiology 75:3634-3640

Lee S, Fuhrman JA (1987) Relationships between biovolume and biomass of naturally derived marine bacterioplankton. Applied Environmental Microbiology 53:1298-1303

Lennon JT, Khatana SAM, Marston MF, Martiny JBH (2007) Is there a cost of virus resistance in marine cyanobacteria? ISME Journal 1:300-312

Lin C-H, Chen Y-C, Pan T-M (2011) Quantification bias caused by plasmid DNA conformation in quantitative real-time PCR assay. PLOS One 6:e29101

Lin Y, Gazsi K, Lance VP, Larkin A, Chandler J, Zinser ER, Johnson ZI (2013) In situ activity of a dominant *Prochlorococcus* ecotype (eHL-II) from rRNA content and cell size. Environmental Microbiology 10:2736-27347

Lindell D, Jaffe JD, Johnson ZI, Church GM, Chisholm SW (2005) Photosynthesis genes in marine viruses yield proteins during host infection. Nature 438:86-89

Lindell D, Sullivan MB, Johnson ZI, Tolonen AC, Rohwer F, Chisholm SW (2004) Transfer of photosynthesis genes to and from *Prochlorococcus* viruses. Proceedings of the National Academy of Sciences of the United States of America 101:11013-11018

Llabres M, Agusti S, Alonso-Laita P, Herndl GJ (2010) *Synechococcus* and *Prochlorococcus* cell death induced by UV radiation and the penetration of lethal UVR in the Mediterranean Sea. Marine Ecology Progress Series 399:27-37

Los M, Wegrzyn G, Neubauer P (2003) A role for bacteriophage T4 rI gene function in the control of phage development during pseudolysogeny and in slowly growing host cells. Research in Microbiology 154:547-552

Maniloff J, Ackermann HW (1998) Taxonomy of bacterial viruses: Establishment of tailed virus genera and the order *Caudovirales*. Archives of Virology 143:2051-2063

Mann NH (2003) Phages of the marine cyanobacterial picophytoplankton. FEMS Microbiology Reviews 27:17-34

Marie D, Partensky F, Jacquet S, Vaulot D (1997) Enumeration and cell cycle analysis of natural populations of marine picoplankton by flow cytometry using the nucleic acid stain SYBR Green I. Applied Environmental Microbiology 63:186-193

Marston MF, Pierciey FJ, Shepard A, Gearin G, Qi J, Yandava C, Schuster SC, Henn MR, Martiny JBH (2012) Rapid diversification of coevolving marine *Synechococcus* and a virus. Proceedings of the National Academy of Sciences of the United States of America 109:4544-4549

Matteson AR, Loar SN, Bourbonniere RA, Wilhelm SW (2011) Molecular enumeration of an ecologically important cyanophage in a Laurentian Great Lake. Applied Environmental Microbiology 77:6772-6779

Matteson AR, Loar SN, Pickmere S, DeBruyn JM, Ellwood MJ, Boyd PW, Hutchins DA, Wilhelm SW (2012) Production of viruses during a spring phytoplankton bloom in the South Pacific Ocean near of New Zealand. FEMS Microbiology Ecology 79:709-719

Matteson AR, Rowe JM, Ponsero AJ, Pimentel TM, Boyd PW, Wilhelm SW (2013) High abundances of cyanomyoviruses in marine ecosystems demonstrate ecological relevance. FEMS Microbiology Ecology:12

McDaniel L, Houchin LA, Williamson SJ, Paul JH (2002) Plankton blooms - lysogeny in marine *Synechococcus*. Nature 415:496-496

Millard A, Clokie MRJ, Shub DA, Mann NH (2004) Genetic organization of the psbAD region in phages infecting marine *Synechococcus* strains. Proceedings of the National Academy of Sciences of the United States of America 101:11007-11012

Millard AD, Mann NH (2006) A temporal and spatial investigation of cyanophage abundance in the Gulf of Aqaba, Red Sea. Journal of the Marine Biological Association of the United Kingdom 86:507-515

Moisa I, Sotropa E, Velehorschi V (1981) Investigations on the presence of cyanophages in fresh and sea waters of Romania. Virologie 32:127-132

Morel A, Ahn YH, Partensky F, Vaulot D, Claustre H (1993) *Prochlorococcus* and *Synechococcus* - a comparative study of their optical properties in relation to their size and pigmentation. Journal of Marine Research 51:617-649

Morel A, Antoine D, Babin M, Dandonneau Y (1996) Measured and modeled primary production in the northeast Atlantic (EUMELI JGOFS program): The impact of natural variations in photosynthetic parameters on model predictive skill. Deep-Sea Research Part I-Oceanographic Research Papers 43:1273-1304

Morrison TB, Weis JJ, Wittwer CT (1998) Quantification of low-copy transcripts by continuous SYBR (R) green I monitoring during amplification. Biotechniques 24:954-+

Muhling M, Fuller NJ, Millard A, Somerfield PJ, Marie D, Wilson WH, Scanlan DJ, Post AF, Joint I, Mann NH (2005) Genetic diversity of marine *Synechococcus* and co-occurring cyanophage communities: evidence for viral control of phytoplankton. Environmental Microbiology 7:499-508

Murray AG, Jackson GA (1992) Viral dynamics - a model of the effects of size, shape, motion and abundance of single-celled planktonic organisms and other particles. Marine Ecology Progress Series 89:103-116

Noble RT, Fuhrman JA (1997) Virus decay and its causes in coastal waters. Applied Environmental Microbiology 63:77-83

Oldham AL, Duncan KE (2012) Similar gene estimates from circular and linear standards in quantitative PCR analyses using the prokaryotic 16S rRNA gene as a model. PLOS One 7

Ortmann AC, Lawrence JE, Suttle CA (2002) Lysogeny and lytic viral production during a bloom of the cyanobacterium *Synechococcus* spp. Microbial Ecology 43:225-231

Ortmann AC, Suttle CA (2009) Determination of virus abundance by epifluorescence microscopy. Methods in Molecular Biology (Clifton, NJ) 501:87-95

Parsons RJ, Breitbart M, Lomas MW, Carlson CA (2012) Ocean time-series reveals recurring seasonal patterns of virioplankton dynamics in the northwestern Sargasso Sea. ISME Journal 6:273-284

Partensky F, Hess WR, Vaulot D (1999) *Prochlorococcus*, a marine photosynthetic prokaryote of global significance. Microbiology and Molecular Biology Reviews 63:106-+

Paul JH (2008) Prophages in marine bacteria: Dangerous molecular time bombs or the key to survival in the seas? ISME Journal 2:579-589

Paul JH, Sullivan MB, Segall AM, Rohwer F (2002) Marine phage genomics. Comparative Biochemistry and Physiology B-Biochemistry & Molecular Biology 133:463-476

Prezelin BB, Glover HE, Campbell L (1987) Effects of light-intensity and nutrient availability on diel patterns of cell-metabolism and growth in populations of *Synechococcus* spp. Marine Biology 95:469-480

Proctor LM, Fuhrman JA (1990) Viral mortality of marine-bacteria and cyanobacteria. Nature 343:60-62

Ritchie RJ (2006) Consistent sets of spectrophotometric chlorophyll equations for acetone, methanol and ethanol solvents. Photosynthesis Research 89:27-41

Rodriguez-Brito B, Li L, Wegley L, Furlan M, Angly F, Breitbart M, Buchanan J, Desnues C, Dinsdale E, Edwards R, Felts B, Haynes M, Liu H, Lipson D, Mahaffy J, Belen Martin-Cuadrado A, Mira A, Nulton J, Pasic L, Rayhawk S, Rodriguez-Mueller J, Rodriguez-Valera F, Salamon P, Srinagesh S, Thingstad TF, Tran T, Thurber RV, Willner D, Youle M, Rohwer F (2010) Viral and microbial community dynamics in four aquatic environments. ISME Journal 4:739-751

Rohwer F, Thurber RV (2009) Viruses manipulate the marine environment. Nature 459:207-212

Rowe JM, DeBruyn JM, Poorvin L, LeCleir GR, Johnson ZI, Zinser ER, Wilhelm SW (2012) Viral and bacterial abundance and production in the western Pacific Ocean and the relation to other oceanic realms. FEMS Microbiology Ecology 79:359-370

Rusch DB, Halpern AL, Sutton G, Heidelberg KB, Williamson S, Yooseph S, Wu D, Eisen JA, Hoffman JM, Remington K, Beeson K, Tran B, Smith H, Baden-Tillson H, Stewart C,

Thorpe J, Freeman J, Andrews-Pfannkoch C, Venter JE, Li K, Kravitz S, Heidelberg JF, Utterback T, Rogers Y-H, Falcon LI, Souza V, Bonilla-Rosso G, Eguiarte LE, Karl DM, Sathyendranath S, Platt T, Bermingham E, Gallardo V, Tamayo-Castillo G, Ferrari MR, Strausberg RL, Nealson K, Friedman R, Frazier M, Venter JC (2007) The Sorcerer II Global Ocean Sampling expedition: Northwest Atlantic through eastern tropical Pacific. PLOS Biology 5:398-431

Safferman RS, Morris ME (1963) Algal virus - isolation. Science 140:679-&

Sandaa R-A, Gomez-Consarnau L, Pinhassi J, Riemann L, Malits A, Weinbauer MG, Gasol JM, Thingstad TF (2009) Viral control of bacterial biodiversity - evidence from a nutrient-enriched marine mesocosm experiment. Environmental Microbiology 11:2585-2597

Sandaa R-A, Larsen A (2006) Seasonal variations in virus-host populations in Norwegian coastal waters: Focusing on the cyanophage community infecting marine *Synechococcus* spp. Applied Environmental Microbiology 72:4610-4618

Schneider RJ, Shenk T (1987) Impact of virus-infection on host-cell protein synthesis. Annual Review of Biochemistry 56:317-332

Sharon I, Alperovitch A, Rohwer F, Haynes M, Glaser F, Atamna-Ismaeel N, Pinter RY, Partensky F, Koonin EV, Wolf YI, Nelson N, Beja O (2009) Photosystem I gene cassettes are present in marine virus genomes. Nature 461:258-262

Sherman LA, Pauw P (1976) Infection of *Synechococcus*-cedrorum by cyanophage AS-1M. 2. Protein and DNA synthesis. Virology 71:17-27

Short CM, Suttle CA (2005) Nearly identical bacteriophage structural gene sequences are widely distributed in both marine and freshwater environments. Applied Environmental Microbiology 71:480-486

Stingl U, Desiderio RA, Cho J-C, Vergin KL, Giovannoni SJ (2007) The SAR92 clade: An abundant coastal clade of culturable marine bacteria possessing proteorhodopsin. Applied Environmental Microbiology 73:2290-2296

Stoddard LI, Martiny JBH, Marston MF (2007) Selection and characterization of cyanophage resistance in marine *Synechococcus* strains. Applied Environmental Microbiology 73:5516-5522

Sullivan MB, Coleman ML, Quinlivan V, Rosenkrantz JE, DeFrancesco AS, Tan G, Fu R, Lee JA, Waterbury JB, Bielawski JP, Chisholm SW (2008) Portal protein diversity and phage ecology. Environmental Microbiology 10:2810-2823

Sullivan MB, Coleman ML, Weigele P, Rohwer F, Chisholm SW (2005) Three *Prochlorococcus* cyanophage genomes: Signature features and ecological interpretations. PLOS Biology 3:790-806

Sullivan MB, Huang KH, Ignacio-Espinoza JC, Berlin AM, Kelly L, Weigele PR, DeFrancesco AS, Kern SE, Thompson LR, Young S, Yandava C, Fu R, Krastins B, Chase M, Sarracino D, Osburne MS, Henn MR, Chisholm SW (2010) Genomic analysis of oceanic cyanobacterial myoviruses compared with T4-like myoviruses from diverse hosts and environments. Environmental Microbiology 12:3035-3056

Sullivan MB, Krastins B, Hughes JL, Kelly L, Chase M, Sarracino D, Chisholm SW (2009) The genome and structural proteome of an ocean siphovirus: A new window into the cyanobacterial 'mobilome'. Environmental Microbiology 11:2935-2951

Sullivan MB, Waterbury JB, Chisholm SW (2003) Cyanophages infecting the oceanic cyanobacterium *Prochlorococcus*. Nature 424:1047-1051

Suttle CA (2000) Ecological, evolutionary, and geochemical consequences of viral infection of cyanobacteria and eukaryotic algae. Viral Ecology 248-286

Suttle CA (2005) Viruses in the sea. Nature 437:356-361

Suttle CA, Chan AM (1993) Marine cyanophages infecting oceanic and coastal strains of *Synechococcus* - abundance, morphology, cross-infectivity and growth-characteristics. Marine Ecology-Progress Series 92:99-109

Suttle CA, Chan AM (1994) Dynamics and distribution of cyanophages and their effect on marine *Synechococcus* spp. Applied Environmental Microbiology 60:3167-3174

Suttle CA, Chan AM, Cottrell MT (1990) Infection of phytoplankton by viruses and reduction of primary productivity. Nature 347:467-469

Suttle CA, Feng C (1992) Mechanisms and rates of decay of marine viruses in seawater. Applied Environmental Microbiology 58:3721-3729

Suttle CA, Fuhrman JA (2010) Enumeration of virus particles in aquatic or sediment samples by epifluorescence microscopy. ASLO:145-153

Thingstad TF, Heldal M, Bratbak G, Dundas I (1993) Are viruses important partners in pelagic food webs? Trends in Ecology & Evolution 8:209-213

Thingstad TF, Lignell R (1997) Theoretical models for the control of bacterial growth rate, abundance, diversity and carbon demand. Aquatic Microbial Ecology 13:19-27

Thompson LR, Zeng Q, Kelly L, Huang KH, Singer AU, Stubbe J, Chisholm SW (2011) Phage auxiliary metabolic genes and the redirection of cyanobacterial host carbon metabolism. Proceedings of the National Academy of Sciences of the United States of America 108:E757-E764

Wang G, Murase J, Asakawa S, Kimura M (2010) Unique viral capsid assembly protein gene (*g20*) of cyanophages in the floodwater of a Japanese paddy field. Biology and Fertility of Soils 46:93-102

Wang K, Chen F (2004) Genetic diversity and population dynamics of cyanophage communities in the Chesapeake Bay. Aquatic Microbial Ecology 34:105-116

Wang K, Wommack KE, Chen F (2011) Abundance and distribution of *Synechococcus* spp. and cyanophages in the Chesapeake Bay. Applied Environmental Microbiology 77:7459-7468

Waterbury JB, Valois FW (1993) Resistance to cooccurring phages enables marine *Synechococcus* communities to coexist with cyanophages abundant in seawater. Applied Environmental Microbiology 59:3393-3399

Waterbury JB, Watson SW, Valois FW, Franks DG (1986) Biological and ecological characterization of the marine unicellular cyanobacterium *Synechococcus*. Can Bull Fish Aquatic Sci 214

Weinbauer MG (2004) Ecology of prokaryotic viruses. FEMS Microbiology Reviews 28:127-181

Weinbauer MG, Bonilla-Findji O, Chan AM, Dolan JR, Short SM, Simek K, Wilhelm SW, Suttle CA (2011) *Synechococcus* growth in the ocean may depend on the lysis of heterotrophic bacteria. Journal of Plankton Research 33:1465-1476

Weinbauer MG, Hofle MG (1998) Significance of viral lysis and flagellate grazing as factors controlling bacterioplankton production in a eutrophic lake. Applied Environmental Microbiology 64:431-438

Weinbauer MG, Rassoulzadegan F (2004) Are viruses driving microbial diversification and diversity? Environmental Microbiology 6:1-11

Weinbauer MG, Wilhelm SW, Suttle CA, Pledger RJ, Mitchell DL (1999) Sunlight-induced DNA damage and resistance in natural viral communities. Aquatic Microbial Ecology 17:111-120

Welschmeyer NA (1994) Fluorometric analysis of chlorophyll-*a* in the presence of chlorophyll-*b* and pheopigments. Limnology and Oceanography 39:1985-1992

Wilhelm SW, Carberry MJ, Eldridge ML, Poorvin L, Saxton MA, Doblin MA (2006) Marine and freshwater cyanophages in a Laurentian Great Lake: Evidence from infectivity assays and molecular analyses of *g20* genes. Applied Environmental Microbiology 72:4957-4963

Wilhelm SW, Matteson AR (2008) Freshwater and marine virioplankton: A brief overview of commonalities and differences. Freshwater Biology 53:1076-1089

Wilhelm SW, Suttle CA (1999) Viruses and nutrient cycles in the sea - viruses play critical roles in the structure and function of aquatic food webs. Bioscience 49:781-788

Wilhelm SW, Weinbauer MG, Suttle CA, Jeffrey WH (1998) The role of sunlight in the removal and repair of viruses in the sea. Limnology and Oceanography 43:586-592

Williamson SJ, Rusch DB, Yooseph S, Halpern AL, Heidelberg KB, Glass JI, Andrews-Pfannkoch C, Fadrosh D, Miller CS, Sutton G, Frazier M, Venter JC (2008) The Sorcerer II Global Ocean Sampling expedition: Metagenomic characterization of viruses within aquatic microbial samples. PLOS One 3

Wilson WH, Carr NG, Mann NH (1996) The effect of phosphate status on the kinetics of cyanophage infection in the oceanic cyanobacterium *Synechococcus* sp WH7803. Journal of Phycology 32:506-516

Winter C, Herndl GJ, Weinbauer MG (2004) Diel cycles in viral infection of bacterioplankton in the North Sea. Aquatic Microbial Ecology 35:207-216

Wommack KE, Colwell RR (2000) Virioplankton: Viruses in aquatic ecosystems. Microbiology and Molecular Biology Reviews 64:69-+

Yang Y, Motegi C, Yokokawa T, Nagata T (2010) Large-scale distribution patterns of virioplankton in the upper ocean. Aquatic Microbial Ecology 60:233-246

Yooseph S, Sutton G, Rusch DB, Halpern AL, Williamson SJ, Remington K, Eisen JA, Heidelberg KB, Manning G, Li W, Jaroszewski L, Cieplak P, Miller CS, Li H, Mashiyama ST, Joachimiak MP, van Belle C, Chandonia J-M, Soergel DA, Zhai Y, Natarajan K, Lee S, Raphael BJ, Bafna V, Friedman R, Brenner SE, Godzik A, Eisenberg D, Dixon JE, Taylor SS, Strausberg RL, Frazier M, Venter JC (2007) The Sorcerer II Global Ocean Sampling expedition: Expanding the universe of protein families. PLOS Biology 5:432-466

Zeng Q, Chisholm SW (2012) Marine viruses exploit their host's two-component regulatory system in response to resource limitation. Current Biology 22:124-128

Zhao Y, Temperton B, Thrash JC, Schwalbach MS, Vergin KL, Landry ZC, Ellisman M, Deerinck T, Sullivan MB, Giovannoni SJ (2013) Abundant SAR11 viruses in the ocean. Nature 494:357-360

Zhong Y, Chen F, Wilhelm SW, Poorvin L, Hodson RE (2002) Phylogenetic diversity of marine cyanophage isolates and natural virus communities as revealed by sequences of viral capsid assembly protein gene *g20*. Applied Environmental Microbiology 68:1576-1584

APPENDIX

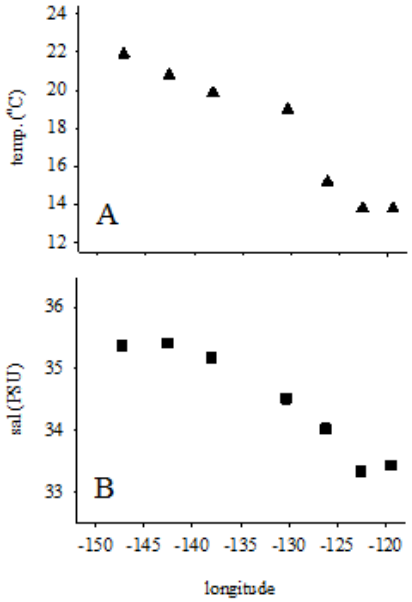

Figure 9. Temperature and salinity across the transect (underway samples). Temperature (A) and salinity (B) were measured by an on-board sensor. The x-axis indicates longitude in degrees east.

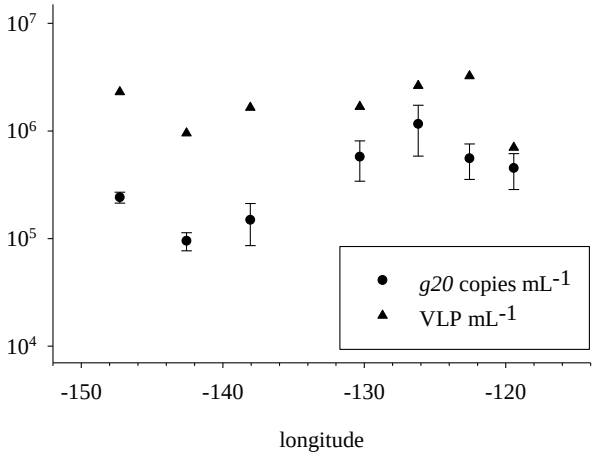

Figure 10. Cyanomyoviral and total viral abundance across the transect (underway samples). The y-axis represents VLP or g20 copies mL^{-1}. The y- axis represents longitude in degrees east. Error bars represent the standard deviation. Where error bars are not visible, they do not exceed the width of the symbol.

VITA

Tiana Pimentel was born in Santa Rosa, CA to her parents Anne Krohn and Robert Pimentel. She has one younger sister named Leah. When she was six years old, her family moved across the country to Asheville, NC, which is where she spent most of her childhood. Tiana attended several elementary schools, but eventually ended up at Haw Creek Elementary and continued on to A.C. Reynolds Middle School and A.C. Reynolds High School. She then acquired a degree in Biology at the University of North Carolina at Wilmington, where she completed a departmental honors project on a novel equine herpes virus-1 (EHV-1) antiviral. She graduated with a B.S. in Biology and minors in Chemistry and Forensic Science in May, 2011. After graduation, she moved to Tennessee to pursue a Master's in Microbiology at the University of Tennessee – Knoxville, where she currently resides with her long-term boyfriend, Nick. Her three birds, a cockatiel (Olive) and two parakeets (Phillip and Chester), keep her entertained with their respective idiosyncrasies.